Mechanistic Studies of Pd(II)−α-Diimine-Catalyzed Olefin Polymerizations[1]

Daniel J. Tempel,[†] Lynda K. Johnson,[‡] R. Leigh Huff, Peter S. White, and Maurice Brookhart*

Department of Chemistry, University of North Carolina at Chapel Hill, CB#3290, Chapel Hill, North Carolina 27599-3290

Received March 13, 2000

Abstract: Mechanistic studies of olefin polymerizations catalyzed by aryl-substituted α-diimine−Pd(II) complexes are presented. Syntheses of several cationic catalyst precursors, $[(N\hat{}N)Pd(CH_3)(OEt_2)]BAr'_4$ ($N\hat{}N$ = aryl-substituted α-diimine, Ar′ = 3,5-$(CF_3)_2C_6H_3$), are described. X-ray structural analyses of [ArN═C(H)C(H)═NAr]Pd(CH_3)(Cl) and [ArN═C(Me)C(Me)═NAr]Pd$(CH_3)_2$ (Ar = 2,6-(*i*Pr)$_2C_6H_3$) illustrate that *o*-aryl substituents crowd axial sites in these square planar complexes. Low-temperature NMR studies show that the alkyl olefin complexes, $(N\hat{}N)Pd(R)(olefin)^+$, are the catalyst resting states and that the barriers to migratory insertions lie in the range 17−19 kcal/mol. Following migratory insertion, the cationic palladium alkyl complexes $(N\hat{}N)Pd(alkyl)^+$ formed are *β*-agostic species which exhibit facile metal migration along the chain ("chain walking") via *β*-hydride elimination/readdition reactions. Model studies using palladium−*n*-propyl and −isopropyl systems provide mechanistic details of this process, which is responsible for introducing branching in the polyethylenes made by these systems. Decomposition of the cationic methyl complexes $(ArN\hat{}NAr)Pd(CH_3)(OEt_2)^+$ (Ar = 2,6-(*i*Pr)$_2C_6H_3$, 2-*t*BuC_6H_4) occurs by C−H activation of *β*-C−H bonds of the ortho isopropyl and *tert*-butyl substituents and loss of methane. The rate of associative exchange of free ethylene with bound ethylene in $(N\hat{}N)Pd(CH_3)(C_2H_4)^+$ is retarded by bulky substituents. The relationship of these exchange experiments to chain transfer is discussed.

Introduction

Prior to reports from these laboratories, a few Ni(II)-based catalysts were known to polymerize ethylene to linear polyethylene.[2−9] Due to rapid chain transfer, dimerization and oligomerization reactions of ethylene[4,10−16] and α-olefins[17] were the most commonly reported features of late metal catalysts. We have described a family of cationic palladium(II) and nickel(II) complexes bearing bulky aryl-substituted α-diimine ligands which are capable of polymerizing ethylene, α-olefins, and internal and cyclic olefins to high molar mass polymers.[18] Polymerizations of common, inexpensive monomers using these catalysts result in the formation of unique materials including highly branched, amorphous polyethylene, "chain-straightened" poly(α-olefins), and melt processable polycyclopentene.[18−30] In

[†] Current address: Air Products and Chemicals, Inc. Allentown, PA 18195-1501.

[‡] Current address: E. I. DuPont and Co., Central Research and Development, Wilmington, DE 19880-0328.

(1) This paper has been adapted, in part, from the following thesis: Tempel, D. J. Ph.D. Dissertation, University of North Carolina at Chapel Hill, 1998.

(2) Keim, W.; Appel, R.; Storeck, A.; Kruger, C.; Goddard, R. *Angew. Chem., Int. Ed. Engl.* **1981**, *20*, 116−117.

(3) Klabunde, U.; Ittel, S. D. *J. Mol. Catal.* **1987**, *41*, 123−134.

(4) Wilke, G. *Angew. Chem., Int. Ed. Engl.* **1988**, *27*, 185−206.

(5) Keim, W.; Kowaldt, F. H.; Goddard, R.; Kruger, C. *Angew. Chem., Int. Ed. Engl.* **1978**, *17*, 466.

(6) Keim, W. *Angew. Chem., Int. Ed. Engl.* **1990**, *29*, 235.

(7) Ostoja Starzewski, K. A.; Witte, J. *Angew. Chem.* **1985**, *97(7)*, 610−612.

(8) Ostoja Starzewski, K. A.; Witte, J.; Reichert, K. H.; Vasiliou, G. In *Transition Met. Organomet. Catal. Olefin Polym., [Proc. Int. Symp.]*. Kaminsky, W., Sinn, H., Eds.; Springer: Berlin, 1988; pp 349−360.

(9) For additional references, see: (a) Johnson, L. K.; Killian, C. M. In *Metallocene-Based Polyolefins: Preparation, Properties, and Technology*; Scheirs, J., Kaminsky, W., Eds.; Wiley: West Sussex, 2000; p 233. (b) Ittel, S. D. In *Metalorganic Catalysts for Synthesis and Polymerization*; Kaminsky, W., Ed.; Springer-Verlag: Heidelberg, 1999; p 616.

(10) Keim, W.; Behr, A.; Limbacker, B.; Kruger, C. *Angew. Chem., Int. Ed. Engl.* **1983**, *22*, 503.

(11) Peuckert, M.; Keim, W. *Organometallics* **1983**, *2*, 594−597.

(12) Cavell, K. J.; Masters, A. F. *Aust. J. Chem.* **1986**, *39*, 1129−1134.

(13) Rix, F. C.; Brookhart, M. *J. Am. Chem. Soc.* **1995**, *117*, 1137−1138.

(14) Desjardins, S. Y.; Cavell, K. J.; Jin, H.; Skelton, B. W.; White, A. H. *J. Organomet. Chem.* **1996**, *515*, 233−243.

(15) Desjardins, S. Y.; Cavell, K. J.; Hoare, J. L.; Skelton, B. W.; Sobolev, A. N.; White, A. H.; Keim, W. *J. Organomet. Chem.* **1997**, *544*, 163−174.

(16) Svedja, S. A.; Brookhart, M. *Organometallics* **1999**, *18*, 65−74 and extensive references therein.

(17) Certain Ni(II) species have been reported which convert α-olefins to oligomers with DP's of ∼4−20. A chain-walking mechanism was proposed to account for the oligomer microstructures observed: (a) Möhring, V. M.; Fink, G. *Angew. Chem., Int. Ed. Engl.* **1985**, *24*, 1001−1003 (b) Schubbe, R.; Angermund, K.; Fink, G.; Goddard, R. *Makromol. Chem. Phys.* **1995**, *196*, 467−468.

(18) Johnson, L. K.; Killian, C. M.; Brookhart, M. *J. Am. Chem. Soc.* **1995**, *117*, 6414−6415.

(19) Killian, C. M. Ph.D. Dissertation, University of North Carolina at Chapel Hill, 1996.

(20) Brookhart, M. S.; Johnson, L. K.; Killian, C. M.; Arthur, S. D.; Feldman, J.; McCord, E. F.; McLain, S. J.; Kreutzer, K. A.; Bennett, A. M. A.; Coughlin, E. B.; Ittel, S. D.; Parthasarathy, A.; Tempel, D. J. WO 9623010, 1996.

(21) McLain, S. J.; Feldman, J.; McCord, E. F.; Gardner, K. H.; Teasley, M. F.; Coughlin, E. B.; Sweetman, K. J.; Johnson, L. K.; Brookhart, M. *Macromolecules* **1998**, *31*, 6705−6707.

(22) Killian, C. M.; Tempel, D. J.; Johnson, L. K.; Brookhart, M. *J. Am. Chem. Soc.* **1996**, *118*, 11664−11665.

(23) Thompson, D. T. *Plat. Metals Rev.* **1996**, *40*, 78−79.

(24) Killian, C. M.; Johnson, L. K.; Brookhart, M. *Organometallics* **1997**, *16*, 2005−2007.

(25) Johnson, L. K.; Killian, C. M. In *Metallocene-Based Polyolefins: Preparation, Properties, and Technology*; Scheirs, J., Kaminsky, W., Eds.; Wiley: West Sussex, 2000; p 233.

10.1021/ja000893v CCC: $19.00
Published on Web 06/30/2000

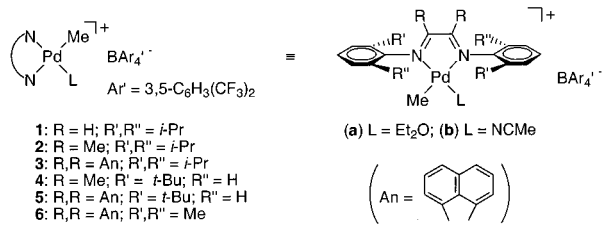

Figure 1. Palladium−α-diimine complexes used as olefin polymerization catalysts.

addition, the palladium−α-diimine catalysts are the first transition metal complexes reported which are capable of copolymerizing ethylene and α-olefins with functionalized monomers such as alkyl acrylates and methyl vinyl ketone.[20,31,32] Following our initial reports of these catalysts, other groups have described similar results using α-diimine-based systems.[33−40] Neutral, bidentate Ni(II) systems which incorporate bulky aryl-substituted imine units have also recently been shown to be quite effective for polymerization of ethylene to high molecular weight polymers.[41−43]

In contrast to the extremely active, highly air-sensitive nickel analogues,[18,44] the well-defined cationic palladium−alkyl species depicted in Figure 1 are more easily synthesized and handled and exhibit rates of reaction that make them well-suited for study using variable temperature NMR spectroscopic techniques. On the basis of our initial NMR observations and analyses of polymer microstructures, we proposed the polymerization mechanism shown in Schemes 1A and 1B(i) (illustrated here for the case of ethylene polymerization).

The overall mechanism of polymerization consists of three main processes beyond initiation: (1) chain propagation, (2) metal migration along the polymer chain ("chain running"), and (3) chain transfer. The first and third processes are common to all ethylene oligomerization and polymerization catalysts. Metal migration, on the other hand, is insignificant for most catalytic systems[17,45,46] but is a major reaction pathway for the Pd−α-diimine catalysts, thus making chain-running the most distinguishing feature of these systems. For acyclic olefins, the resting states of the palladium catalysts have been observed by NMR spectroscopy to be alkyl−olefin complexes. In the absence of excess olefin or other Lewis bases, the alkyl cations exist as stable β-agostic species.[44,47−49] A β-agostic alkyl species is observed to be the resting state for cyclopentene polymerizations.[21]

Propagation and isomerization (Scheme 1A) are easily monitored by low-temperature NMR spectroscopy in this system. Insertion of ethylene from the catalyst resting state **7** produces the linear alkyl agostic species **8**, which can be trapped by free ethylene. Repetition of this cycle (**7** → **8** → **7**) results in the growth of a linear polymer chain. Complex **8** can also β-hydride eliminate and reinsert with opposite regiochemistry to produce the branched β-agostic species **10**. This process may involve an alkyl−olefin intermediate, **9**, though such a species has never been observed in this system. The branched alkyl

Scheme 1. Proposed Mechanism for Ethylene Polymerization

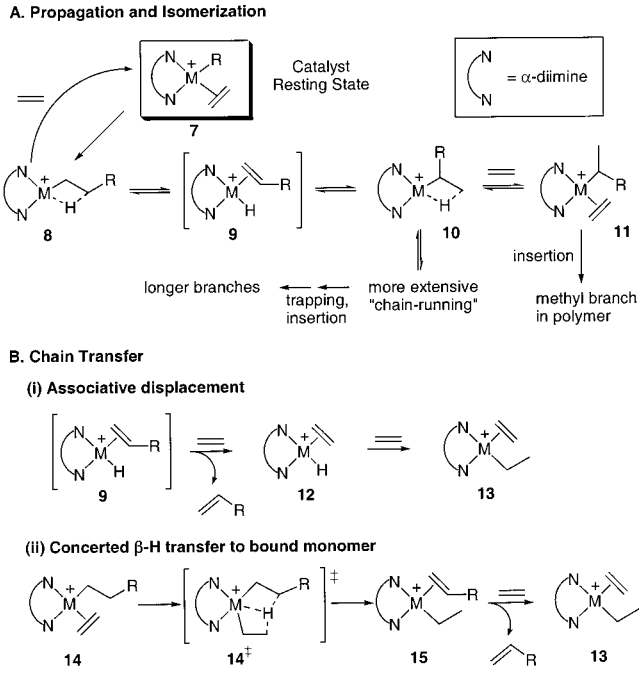

(26) Ittel, S. D. In *Metalorganic Catalysts for Synthesis and Polymerization*; Kaminsky, W., Eds.; Springer-Verlag: Heidelberg, 1999; p 616.
(27) Guan, Z. B.; Cotts, P. M.; McCord, E. F.; McLain, S. J. *Science* **1999**, *283*, 2059−2062.
(28) McLain, S. J.; McCord, E. F.; Johnson, L. K.; Ittel, S. D.; Nelson, L. T. J.; Arthur, S. D.; Halfhill, M. J.; Teasley, M. F.; Tempel, D. J.; Killian, C.; Brookhart, M. *Polym. Prepr. (Am. Chem. Soc., Div. Polym. Chem.)* **1997**, *38(1)*, 772−773.
(29) Guan, Z. B.; Cotts, P. M.; McCord, E. F.; McLain, S. J. *Polym. Prepr. (Am. Chem. Soc., Div. Polym. Chem.)* **1998**, *39(2)*, 402−403.
(30) Guan, Z. B. *Polym. Mater. Sci. Eng.* **1999**, *80*, 50.
(31) Johnson, L. K.; Mecking, S.; Brookhart, M. *J. Am. Chem. Soc.* **1996**, *118*, 267−268.
(32) Mecking, S.; Johnson, L. K.; Wang, L.; Brookhart, M. *J. Am. Chem. Soc.* **1998**, *120*, 888−899.
(33) Galland, G. B.; de Souza, R. F.; Mauler, R. S.; Nunes, F. F. *Macromolecules* **1999**, *32*, 1620−1625.
(34) Heinemann, J.; Mülhaupt, R.; Brinkmann, P.; Luinstra, G. *Macromol. Chem. Phys.* **1999**, *200*, 384−389.
(35) Eilerts, N. W. WO 9915569, 1999.
(36) Jurkiewicz, A.; Eilerts, N. W.; Hsieh, E. T. *Macromolecules* **1999**, *32*, 5471−5476.
(37) Schleis, T.; Heinemann, J.; Spaniol, T. P.; Mulhaupt, R.; Okuda, J. *Inorg. Chem. Commun.* **1998**, *1*, 431−434.
(38) Schleis, T.; Spaniol, T. P.; Okuda, J.; Heinemann, J.; Mulhaupt, R. *J. Organomet. Chem.* **1998**, *569*, 159−167.
(39) Pappalardo, D.; Mazzeo, M.; Pellechia, C. *Macromol. Rapid Commun.* **1997**, *18(12)*, 1017.
(40) For recent reviews of late metal polymerization catalysts, see: (a) Britovsek, G. J. P.; Gibson, V. C.; Kimberly, B. S.; Maddox, P. J.; McTravish, S. J.; Solan, G. A.; White, A. J. P.; Williams, D. J. *Chem. Commun.* **1998**, 849−850 (b) Piccolini, R. J. *ChemTech* **1999**, *29(5)*, 39−40 (c) Thompson, D. T. *Plat. Metals Rev.* **1996**, *40*, 78−79.
(41) Johnson, L. K.; Bennett, A. M. A.; Ittel, S. D.; Wang, L.; Parthasarathy, A.; Hauptman, E.; Simpson, R. D.; Feldman, J.; Coughlin, E. B. WO 9830609, 1997.
(42) Wang, C.; Friedrich, S.; Younkin, T. R.; Li, R. T.; Grubbs, R. H.; Bansleben, D. A.; Day, M. W. *Organometallics* **1998**, *17*, 3149−3151.
(43) Younkin, T. R.; Connor, E. F.; Henderson, J. I.; Friedrich, S. K.; Grubbs, R. H.; Bansleben, D. A. *Science* **2000**, *287*, 460−462.
(44) Svejda, S. A.; Johnson, L. K.; Brookhart, M. *J. Am. Chem. Soc.* **1999**, *121*, 10634−10635.
(45) Exceptions for homopolyethylene (4−12 branches/1000C) include: (a) Karol, F. J.; Karapinka, G. L.; Wu, C.; Dow, A. W.; Johnson, R. N.; Carrick, W. L. *J. Polym. Sci., A-1* **1972**, *10*, 2621−2637 (b) Karol, F. J.; Johnson, R. N. *J. Polym. Sci., Polym. Chem. Ed.* **1975**, *13*, 1607−1617.
(46) Exceptions for poly(α-olefins) include: (a) Rieger, B.; Mu, X.; Mallin, D. T.; Rausch, M. D.; Chien, J. C. W. *Macromolecules* **1990**, *23*, 3559−3568. (b) Soga, K.; Shiono, R.; Takemura, S.; Kaminsky, W. *Makromol. Chem. Rapid Commun.* **1987**, *8*, 305−310. (c) Spalek, W.; Antberg, M.; Aulbach, M.; Bachmann, B.; Dolle, V.; Haftka, S.; Kuber, F.; Rohrmann, J.; Winter, A. In *Ziegler Catalysts*; Fink, G., Mülhaupt, R., Brintzinger, H. H., Eds.; Springer: Berlin, 1995; p 83.
(47) Brookhart, M.; Green, M. L. H.; Wong, L.-L. *Prog. Inorg. Chem.* **1988**, *36*, 1−124.
(48) Tempel, D. J.; Brookhart, M. *Organometallics* **1998**, *17*, 2290−2296.
(49) Similar species have been observed previously by Spencer et al.; see, for example: Conroy-Lewis, F. M.; Mole, L.; Redhouse, A. D.; Litster, S. A.; Spencer, J. L. *J. Chem. Soc., Chem. Commun.* **1991**, 1601−1603.

cation **10** can continue to "chain run" by β-hydride elimination and reinsertion with opposite regiochemistry, producing longer branches. Alternatively, **10** can be trapped with ethylene, and insertion produces a polymer chain containing a methyl branch along the backbone. In the case of nickel, trapping and insertion are competitive with chain-running, and thus the extent of branching is dependent on ethylene pressure.[18] For palladium systems, the total number of branches is nearly insensitive to ethylene pressure, but the number of branches-on-branches and the overall architecture of the polymer does vary with ethylene pressure.[20,27] In the case of α-olefins, 2,1-insertion followed by metal migration to the terminal carbon can result in incorporation of α-olefin in a 1,ω (linear) fashion with the resultant polymer containing fewer branches than expected for simple 1,2 monomer enchainment, a phenomenon we term "chain-straightening".[18,20]

Bulky aryl-substituted α-diimine complexes slow the rate of chain transfer relative to propagation, resulting in the formation of high polymer. This rate retardation clearly results from substituting the ortho positions of the aryl rings with bulky substituents which then project into the axial sites of the square planar complexes.[50] The precise mode of chain transfer is not yet completely understood. Initially we proposed that chain transfer occurred by associative displacement of the unsaturated chain from an olefin hydride complex (Scheme 1B(i)), a process slowed by axial bulk. Calculations by Ziegler suggest chain transfer may occur from the alkyl olefin resting state by direct β-hydride transfer to monomer (Scheme 1B(ii)).[51,52]

We describe in this paper mechanistic investigations of olefin polymerizations catalyzed by the well-defined cationic palladium−alkyl complexes depicted in Figure 1. These investigations include NMR spectroscopic characterization of catalyst resting states, measurement of insertion barriers and the effects of substituents on these barriers, determination of the mode and energetics of palladium migration, as well as the nature and relative stabilities of key β-agostic alkyl complexes, and measurement of associative exchange rates in alkyl−olefin complexes which relate to the chain transfer process. These experimental studies are complemented by recent theoretical calculations from other groups concerning various mechanistic details of these catalyst systems.[51−57]

Results and Discussion

Synthesis of Palladium Complexes. Syntheses of the *N*-aryl-substituted α-diimine ligands are straightforward,[58,59] and the properties of α-diimines as ligands for transition metal compounds have been reviewed.[60] The dimethyl precursors to the active catalysts can be approached by several routes (eqs 1−5).

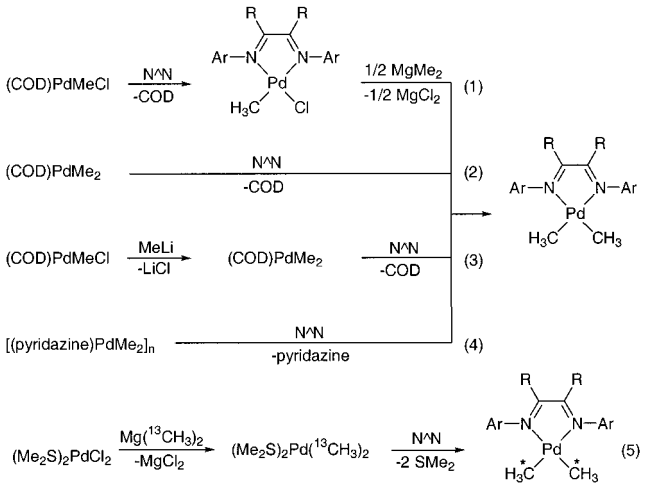

Stable palladium complexes of the general formula (N^N)-PdMeCl are formed in diethyl ether or dichloromethane solvent via displacement of 1,5-cyclooctadiene (COD) from (COD)-PdMeCl by 1 equiv of α-diimine ligand.[61] Subsequent addition of 0.5 equiv of $MgMe_2$ to the product then gives the desired dimethyl complex along with 0.5 equiv of $MgCl_2$ (eq 1). This two-step sequence requires separation of the product from $MgCl_2$ and gives moderate yields.

Single-crystal X-ray structures of (ArN═C(H)C(H)═NAr)-PdMeCl and of (ArN═C(Me)C(Me)═NAr)$PdMe_2$ (Ar = 2,6-C_6H_3-(*i*-Pr)$_2$) were obtained. ORTEP diagrams for these two compounds are included in Figures 2 and 3, respectively, along with selected bond lengths and angles, which are within the standard range for these types of complexes.[50] Included in Figure 2 is a perspective of the molecular structure perpendicular to the square plane of the complex along with selected torsion angles. The two *N*-aryl rings lie roughly 80° and 67° relative to the square plane of the molecule. Comparison with similar molecules in the literature indicates that as the steric bulk of the α-diimine backbone substituents or of the aryl ortho substituents increases, the *N*-aryl rings tend to lie more perpendicular to the square plane of the molecule, and the ortho substituents more effectively block the axial sites.

The synthesis of (COD)$PdMe_2$, a more reactive precursor, has been reported; crystalline material can be isolated at low temperature through addition of methyl cuprate to (COD)$PdCl_2$ followed by workup with aqueous KCN.[62] The (COD)$PdMe_2$ complex is unstable but can be stored at temperatures below ca. −10 °C. It reacts with α-diimines in ether to give nearly quantitative yields of (N^N)$PdMe_2$, and product isolation is straightforward (eq 2). Preparation of (N^N)$PdMe_2$ complexes through in situ generation of (COD)$PdMe_2$ has been reported by Elsevier et al., and we have also found this route to be effective.[63] The desired complexes are obtained upon reaction of 1 equiv of MeLi with (COD)PdMeCl in ether or THF at low temperature, followed by addition of α-diimine. The product must then be extracted from LiCl (eq 3).

Canty reported the preparation of palladium−dimethyl complexes of nitrogen donor ligands via addition of the ligands to either previously isolated (pyridazine)$PdMe_2$ or in situ generated

(50) van Asselt, R.; Elsevier, C. J.; Smeets, W. J. J.; Spek, A. L.; Benedix, R. *Recl. Trav. Chim. Pays-Bas* **1994**, *113*, 88−98.
(51) Deng, L.; Margl, P.; Ziegler, T. *J. Am. Chem. Soc.* **1997**, *119*, 1094−1100.
(52) Deng, L.; Woo, T. K.; Cavallo, L.; Margl, P. M.; Ziegler, T. *J. Am. Chem. Soc.* **1997**, *119*, 6177−6186.
(53) Michalak, A.; Ziegler, T. *Organometallics* **1999**, *18*, 3998−4004.
(54) Woo, T. K.; Ziegler, T. *J. Organomet. Chem.* **1999**, *591*, 204−213.
(55) Stromberg, S.; Zetterberg, K.; Siegbahn, P. E. M. *J. Chem. Soc., Dalton Trans.* **1997**, 4147−4152.
(56) Musaev, D. G.; Svensson, M.; Morokuma, K.; Stromberg, S.; Zetterberg, K.; Siegbahn, P. E. M. *Organometallics* **1997**, *16*, 1933−1945.
(57) Froese, R. D. J.; Musaev, D. G.; Morokuma, K. *J. Am. Chem. Soc.* **1998**, *120*, 1581−1587.
(58) Svoboda, M.; tom Dieck, H. *J. Organomet. Chem.* **1980**, *191*, 321−328.
(59) tom Dieck, H.; Svoboda, M.; Greiser, T. *Z. Naturforsch* **1981**, *36b*, 823−832.
(60) van Koten, G.; Vrieze, K. *Adv. Organomet. Chem.* **1982**, *21*, 151−239.
(61) Rülke, R. E.; Ernsting, J. M.; Spek, A. L.; Elsevier, C. J.; van Leeuwen, P. W. N. M.; Vrieze, K. *Inorg. Chem.* **1993**, *32*, 5769−5778.
(62) Rudler-Chauvin, M.; Rudler, H. *J. Organomet. Chem.* **1977**, *134*, 115−119.
(63) van Asselt, R.; Rijnberg, E.; Elsevier, C. J. *Organometallics* **1994**, *13*, 706−720.

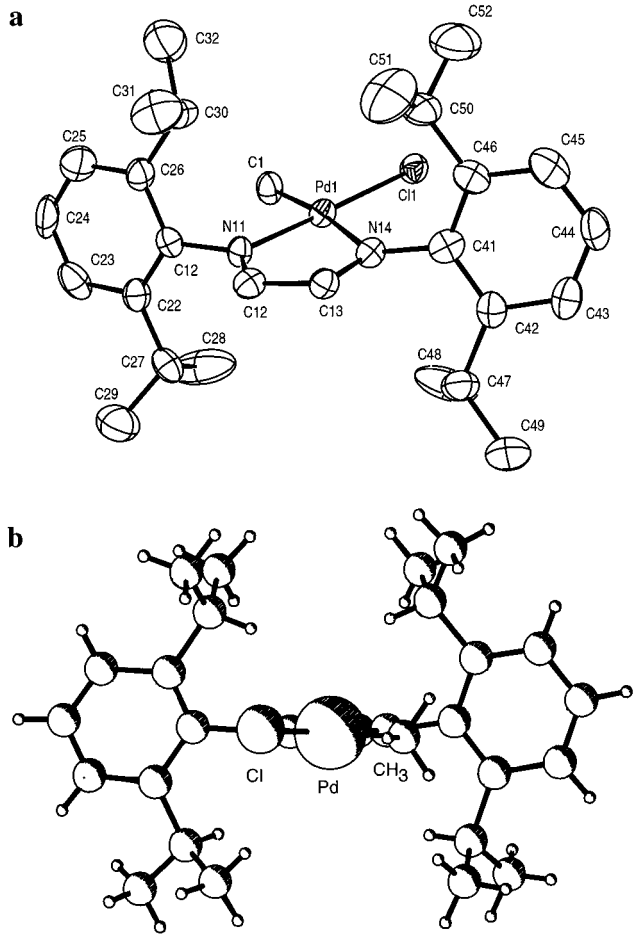

Figure 2. (a) ORTEP diagram of (ArN═C(H)C(H)═NAr)PdMeCl (Ar = 2,6-C_6H_3-(*i*-Pr)$_2$). Selected bond lengths (Å): P(1)−Cl(1) 2.300(4), Pd(1)−C(1) 2.020(11), Pd(1)−N(11) 2.033(9), Pd(1)−N(14) 2.208(9), N(11)−C(12) 1.315(16), N(11)−C(21) 1.448(14), C(12)−C(13) 1.434(17), C(13)−N(14) 1.262(18), N(14)−C(41) 1.450(16). Selected bond angles (deg): Cl(1)−Pd(1)−C(1) 89.7(4), Cl(1)−Pd(1)−N(11) 174.9(3), Cl(1)−Pd(1)−N(14) 99.9(3), C(1)−Pd(1)−N(11) 94.3(4), C(1)−Pd(1)−N(14), N(11)−Pd(1)−N(14) 76.2(4), Pd(1)−N(11)−C(12) 117.6(8), Pd(1)−N(11)−C(21) 124.1(7), C(12)−N(11)−C(21) 118.0(9), Pd(1)−N(14)−C(13) 111.3(8), Pd(1)−N(14)−C(41) 126.2(8), C(13)−N(14)−C(41) 122.5(10), N(11)−C(12)−C(13) 115.3(12), C(12)−C(13)−N(14) 119.5(11), N(11)−C(21)−C(22) 120.8(11), N(11)−C(21)−C(26) 116.2(10), N(14)−C(41)−C(42) 119.5(11), N(14)−C(41)−C(46) 116.2(11). Selected torsion angles (deg): N(11)−C(12)−C(13)−N(14) 1.2(10), C(12)−N(11)−C(21)−C(26) 100.5(21), C(13)−N(14)−C(41)−C(46) −113.5(25). (b) View of the molecular structure perpendicular to the square plane of the complex.

$(Me_2S)_2PdMe_2$.[64] Displacement of pyridazine from the former also occurs for the *N*-aryl α-diimines and gives moderate yields of product in ether solvent (eq 4). α-Diimine displacement of dimethyl sulfide from the in situ generated precursor in ether gives somewhat lower yields of product, but a modification of this route employing $Mg(^{13}CH_3)_2$ proved to be effective for synthesis of a ^{13}C-labeled analogue (eq 5).[48]

Ether adducts of well-defined cationic Pd(II)−α-diimine salts of BAr'_4^- (Ar′ = 3,5-$C_6H_3(CF_3)_2$) are synthesized through addition of $H(OEt_2)_2BAr'_4$ to complexes with the general formula (N^N)Pd$(CH_3)_2$ (eq 6). Through protonolysis, the oxonium acid cleaves one of the Pd−methyl bonds, opening up a coordination site on the metal center through loss of methane. When the reaction is carried out in diethyl ether, one molecule of solvent acts as a Lewis base and occupies the vacant coordination site. The ether ligand is extremely labile, making the precursors ideal for low-temperature NMR mechanistic studies.

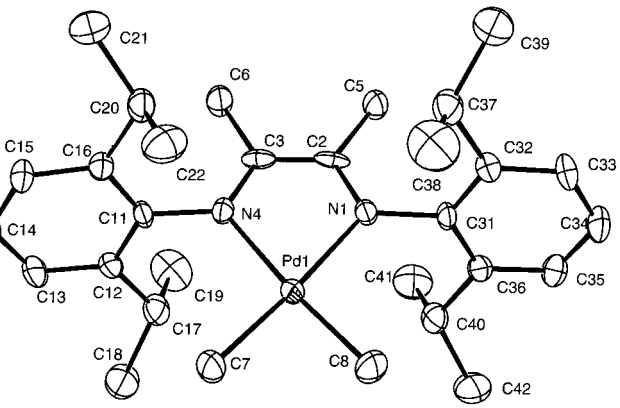

Figure 3. ORTEP diagram of (ArN═C(Me)C(Me)═NAr)PdMe$_2$ (Ar = 2,6-C_6H_3-(*i*-Pr)$_2$). Selected bond lengths (Å): Pd(1)−N(1) 2.133(4), Pd(1)−N(4) 2.145(4), Pd(1)−C(7) 2.023(6), Pd(1)−C(8) 2.033(5), N(1)−C(2) 1.317(6), N(1)−C(31) 1.460(6), C(2)−C(3) 1.366(8), C(2)−C(5) 1.524(7), C(3)−N(4) 1.297(6), C(3)−C(6) 1.528(7), N(4)−C(11) 1.459(6). Selected bond angles (deg): N(1)−Pd(1)−N(4) 74.81(15), N(1)−Pd(1)−C(7) 174.97(19), N(1)−Pd(1)−C(8) 99.55(20), N(4)−Pd(1)−C(7) 100.17(19), N(4)−Pd(1)−C(8) 174.31(20), C(7)−Pd(1)−C(8) 85.47(23), Pd(1)−N(1)−C(2) 114.2(3), Pd(1)−N(1)−C(31) 123.7(3), C(2)−N(1)−C(31) 122.1(4), N(1)−C(2)−C(3) 118.2(4), N(1)−C(2)−C(5) 120.0(5), C(3)−C(2)−C(5) 121.8(4), C(2)−C(3)−N(4) 118.1(4), C(2)−C(3)−C(6) 120.8(4), N(4)−C(3)−C(6) 121.1(5), Pd(1)−N(4)−C(3) 114.7(3), Pd(1)−N(4)−C(11) 121.5(3), C(3)−N(4)−C(11) 123.7(4). Selected torsion angles (deg): N(1)−C(2)−C(3)−N(4) −0.9(3), C(2)−N(1)−C(31)−C(32) 78.6(6), C(3)−N(4)−C(11)−C(16) −79.4(6).

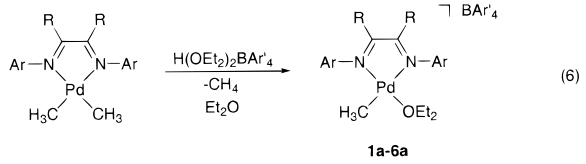

(6)

For preparative-scale polymerizations, complexes in which the vacant coordination site is occupied by a stronger Lewis base than ether are sufficient. For example, an active catalyst is formed in situ upon addition of $NaBAr'_4$ to (N^N)PdMeCl in the presence of olefin. Acetonitrile complexes can be isolated under similar conditions in the absence of olefin, but chloride-bridged, monocationic dimers of the formulas [(N^N)PdMe-μ-Cl]$_2BAr'_4$ are formed when the same reaction is run in diethyl ether. Ether is apparently too weakly coordinating to break open the dimer. Six-membered chelate complexes resulting from acrylate insertion also display activity for olefin homopolymerization and olefin/acrylate copolymerization.[31,32]

The routes described above were found to be ineffective for the preparation of a palladium complex from an α-diimine ligand with an ortho *tert*-butyl group on the ring, e.g., 2-C_6H_4(*t*-Bu)N═C(Me)C(Me)═N-2-C_6H_4(*t*-Bu), and a different approach was required. Addition of $NaBAr'_4$ to (COD)PdMeCl at low temperature in a mixture of CH_2Cl_2 and acetonitrile yields [(COD)PdMeNCMe][BAr'_4].[65] This salt can be used directly or isolated and stored at −30 °C and is stable for extended periods. Displacement of COD by the ortho *tert*-butyl-substituted α-di-

(64) Byers, P. K.; Canty, A. J. *Organometallics* **1990**, *9*, 210−220.

(65) This compound was developed by C. M. Killian, M. Brookhart, and J. Feldman. See Brookhart et al. WO 9623010, 1996 for procedure.

imine occurs for this highly electrophilic precursor to yield the expected acetonitrile adduct, **6b** (eq 7).

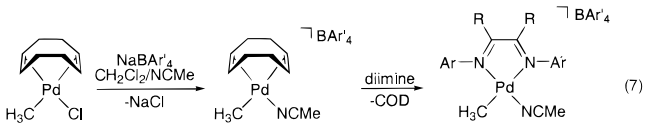

(7)

Catalyst Stability. At room temperature and in the absence of olefin, the cationic acetonitrile adducts are stable for weeks in methylene chloride or chloroform solution. However, under similar conditions solutions of the cationic ether adducts are observed to undergo decomposition via C−H activation of the ortho aryl substituents to give a six-membered palladacycle and methane (eq 8).[66]

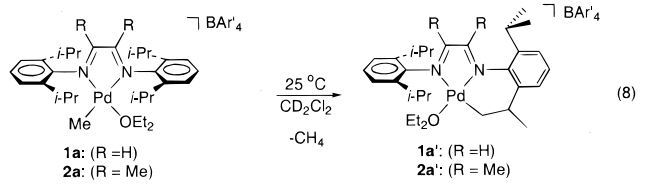

(8)

This intramolecular C−H activation requires one of the ligand aryl rings to rotate into the square plane of the complex. Increasing the steric bulk of the ligand is therefore expected to make this process less favorable, and conversely, the process should become more facile upon decreasing the steric bulk of the ligand. For the reaction indicated in eq 8, changing the backbone substituents from hydrogens to methyl groups results in a significant decrease in rate for the overall process. At 25 °C, the reaction occurs with a half-life of less than 5 min for **1a** (R = H) and a half-life of ca. 30 min for **2a** (R = CH_3) for 0.015 M dichloromethane solutions of these complexes.

Palladacycles **1a′** and **2a′** were not isolated, but complex **1a′** is stable for days as a concentrated dichloromethane solution. In contrast, for the decomposition of ether adduct **2a**, only methane and nonselective decomposition products are observed. The proposed palladacycle **2a′**, if formed, is only a transient intermediate. Presumably, unfavorable steric interactions between the coplanar backbone and the ortho isopropyl substituents make palladacycle **2a′** very unstable.

Addition of ethylene to **1a′** in solution at low temperature results in the formation of an observable ethylene adduct (**1c′**), and addition of an excess of ethylene results in branched polyethylene formation with initiation occurring more slowly than propagation.

The unsymmetrically substituted ether complex **5a** (R,R = An, 0.015 M in CD_2Cl_2) undergoes deactivation with a half-life of ca. 60 min at −3 °C (eq 9) which corresponds to $t_{1/2}$ < 2 min at 25 °C. Therefore, under similar conditions C−H

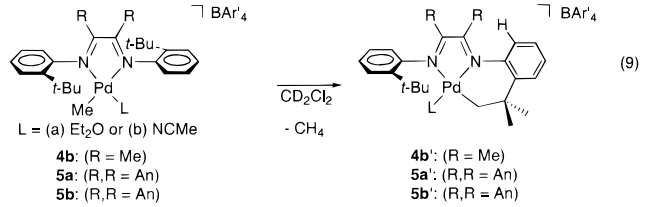

(9)

(66) A similar observation was reported for a square planar *N*-alkyl α-diimine complex of nickel in which intramolecular C−H activation of a ligand methyl group occurs to give a five-membered metallacycle: tom Dieck, H.; Svoboda, M. *Chem. Ber.* **1976**, *109*, 1657−1664.

Scheme 2. Possible Intermediates for Palladacycle Formation via α-Diimine C−H Activation

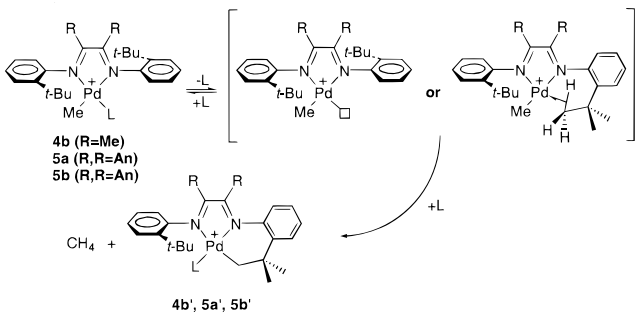

activation of **5a** is more rapid than for **1a** and **2a** and the product, **5a′**, is more stable than both **1a′** and **2a′**. Lack of a highly unfavorable interaction between the ligand backbone and the ortho hydrogen of the in-plane aryl group likely accounts for the rapid activation of **5a** and the relative stability of **5a′**. Introduction of 20 equiv of ethylene to **5a′** leads to displacement of ether to give ethylene-ligated palladacycle **5c′**. However, unlike **1c′**, palladacycle **5c′** exhibits little or no evidence for migratory insertion even after 24 h at room temperature.

The rates of C−H activation of the ether adducts **1a**, **2a**, and **5a** decrease substantially upon addition of an excess of ether. For example, upon addition of 10 equiv of Et_2O to a 0.015 M CD_2Cl_2 solution of **5a** at 0 °C, the C−H activation process is too slow to be monitored over a reasonable time period, and at 10 °C C−H activation occurs with a half-life of more than 1.5 h. One equivalent of acetonitrile readily displaces ether from **5a** to give **5b**, and this complex exhibits only slow deactivation even at room temperature. A 0.015 M solution of the acetonitrile complex **4b** (R = Me; aryl = *o-tert*-butyl) exhibits a half-life for C−H activation of several days at room temperature, and the resulting palladacycle **4b′** has been the most stable complex of this type encountered.

Inhibition of C−H activation by an increased concentration of ether or addition of a stronger Lewis base such as acetonitrile strongly suggests that the C−H activation takes place through an intermediate that is formed reversibly. More specifically, intramolecular activation of a C−H bond of one of the ligand methyl groups likely occurs through initial formation of an agostic interaction between that C−H bond and the metal center (Scheme 2). This mechanism requires displacement of L in order to open up a coordination site for an agostic interaction to form. Displacement of L may occur through a dissociative mechanism involving formation of a 14-electron intermediate, but the possibility also exists that L is displaced associatively by the incoming C−H bond. It is not known whether oxidative addition/reductive elimination or concerted σ-bond metathesis is responsible for completion of the reaction.

Migratory Insertion Rates. In studying the mechanism of olefin polymerization as catalyzed by the palladium α-diimine catalysts, rates for the migratory insertion of olefins were determined using ^{1}H NMR spectroscopy (eq 10). For example,

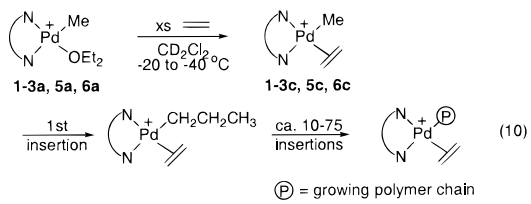

(10)

addition of 10−20 equiv of ethylene to the ether adducts **1a**, **2a**, **3a**, **5a**, and **6a** gave the corresponding methyl ethylene

Table 1. Kinetic Data for Pd-Catalyzed Insertion of Ethylene[a]

	first insertion		subsequent insertions	
catalyst	k_1 ($\times 10^3$ s^{-1})	$\Delta G_1^{\ddagger}$ kcal/mol)	k_{sub} ($\times 10^3$ s^{-1})	$\Delta G_{sub}^{\ddagger}$ (kcal/mol)
1c, −30 °C	1.9	17.2	0.88	17.5
2c, −30 °C	1.7	17.2	3.4	16.9
3c, −26 °C	0.83	17.8	0.67	18.0
5c, −14 °C	2.1	18.3	0.71	18.8
6c, −20 °C	0.63	18.4	0.42	18.6

[a] Error in $\Delta G^{\ddagger}$ measurements is ±0.1 kcal/mol.

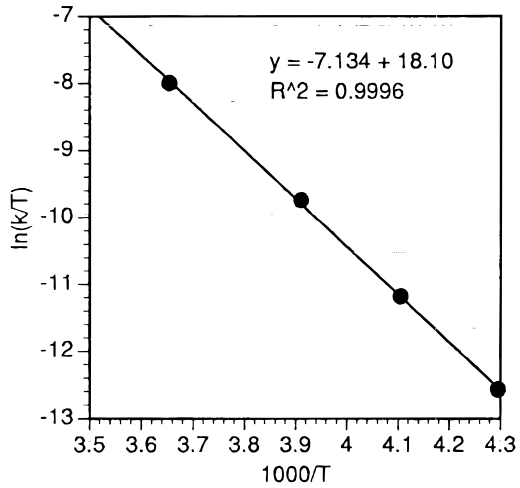

Figure 4. Eyring plot for subsequent ethylene insertions by **2c**.

complexes **1c**, **2c**, **3c**, **5c**, and **6c**. The ensuing first insertion of ethylene into the Pd−methyl bond is first order in catalyst, and the rate for this step is determined by monitoring the decrease of the integral for the Pd-*Me* signal. The combined rate for subsequent insertions is zero order in ethylene and is determined from the turnover frequency based on the decreasing signal for free ethylene in solution. Rates for first and subsequent insertions were used to calculate rate constants and Gibbs free energies of activation (Table 1). For complex **2c**, rate constants for subsequent insertions were obtained over a 40 °C temperature range (−40 to 0 °C). The Eyring plot of the data is shown in Figure 4 and gives $\Delta H^{\ddagger} = 14.2 \pm 0.1$ kcal/mol and $\Delta S^{\ddagger} = -11.2 \pm 0.8$ eu.

The clearest indication of catalyst activity for comparative analysis is the kinetic data for subsequent insertions and more specifically values for $\Delta G_{sub}^{\ddagger}$. The data for the diisopropyl aryl-substituted catalysts **1c**−**3c** indicate that **2c** (R = Me) is the most active for ethylene polymerization, suggesting that ligand steric bulk is the predominant factor affecting the overall rate of polymerization. Increased steric bulk about the metal center likely raises the ground-state energies of the methyl ethylene complexes, resulting in lower barriers to migratory insertion. The *o-tert*-butyl aryl-substituted complex **5c** and the *o*-methyl aryl-substituted complex **6c** exhibit significantly higher barriers to insertion than **1c**−**3c** and are, relatively, poorer catalysts for ethylene polymerization.

Kinetic data for the migratory insertion of propylene using catalysts **2a** and **3a** were collected in a fashion identical to that described for ethylene. The results for these two catalysts are presented in Table 2 and indicate the same trend in activities observed for ethylene insertion. In each case, $\Delta G_{sub}^{\ddagger}$ for propylene propagation increases by 0.5 kcal/mol over $\Delta G_{sub}^{\ddagger}$ determined for ethylene propagation. Importantly, the general trends apparent in Tables 1 and 2 are consistent with what is observed for preparative-scale polymerizations. Namely, for both ethylene and propylene, catalysts based on structure **2** (R = Me) are most active and catalysts based on structures **1** (R = H) and **3** (R,R = An) exhibit fairly similar activities to one another which are lower than activities for **2**.[18] Catalyst **5a** exhibits very few turnovers and gives only low molecular weight polyethylene.

Table 2. Kinetic Data for Pd-Catalyzed Insertion of Propylene[a]

	first insertion		subsequent insertions	
catalyst	k_1 ($\times 10^3$ s^{-1})	$\Delta G_1^{\ddagger}$ (kcal/mol)	k_{sub} ($\times 10^3$ s^{-1})	$\Delta G_{sub}^{\ddagger}$ (kcal/mol)
2a, −30 °C	0.54	17.8	1.2	17.4
3a, −13 °C	1.3	18.6	1.5	18.5

[a] Error in $\Delta G^{\ddagger}$ values is ±0.1 kcal/mol.

Scheme 3. Chain-Running Leading to 1,2-Migration of Palladium

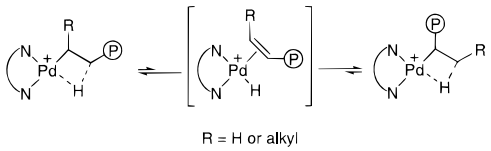

Barriers to insertion in both (N^N)Ni(olefin)R$^+$ and (N^N)-Pd(olefin)R$^+$ species have been theoretically addressed by Ziegler,[51,52] Morokuma,[56,57] and Siegbahn.[55] The calculated barriers for Ni systems invariably fall below those of the corresponding Pd systems, in agreement with experimental observations.[44] In addition, moving from model systems of the type (HN═C(H)C(H)═NH)M(olefin)R$^+$ to systems bearing bulky ortho-disubstituted aryl groups and substituted backbone positions (ArN═C(R′)C(R′)═NAr)M(olefin)R$^+$, the calculated barriers decrease,[51,52] which is consistent with the observations above that bulkier ortho aryl substituents cause a decrease in the migratory insertion barrier. There is reasonable quantitative agreement between the barriers calculated for bulky aryl−palladium diimine systems and the barriers measured in this work. For example, Morokuma[57] has calculated a barrier for insertion of 14.1 kcal/mol for complex **2c** in which the experimentally measured barrier is 17.2 kcal/mol.

Alkyl Intermediates. The number of alkyl branches observed for polyethylene made using a particular Pd−α-diimine catalyst is relatively independent of reaction conditions including temperature, ligand structure, and ethylene concentration, although the type of branches or polymer architecture observed is dependent upon these variables.[18,20,21,27,31,32,36] Polyethylene samples made with the 2,6-diisopropyl-substituted catalysts (structures **1**−**3**) typically exhibit ca. 100−120 branches for every 1000 carbons. This is in sharp contrast to MAO-activated nickel analogues which can be fine-tuned by choice of reaction conditions to give polyethylene ranging in structure from almost completely linear to moderately branched.

As previously described, polyethylene branching arises from facile β-hydride elimination and reinsertion of Pd−alkyl intermediates (chain-running). An olefin−hydride intermediate[67] resulting from β-hydride elimination of a Pd−alkyl species may reinsert with opposite regiochemistry to give a new alkyl complex (Scheme 3). A branch is incorporated into the polymer every time ethylene insertion occurs from any alkyl intermediate other than a primary Pd−alkyl olefin species. Characterization by ^{13}C NMR spectroscopy of polyethylene prepared from

(67) We describe here a discrete olefin−hydride intermediate; however, β-H transfer may occur through a concerted process with an olefin−hydride-like transition state, as suggested by Ziegler et al.: (a) Deng, L.; Margl, P.; Ziegler, T. *J. Am. Chem. Soc.* **1997**, *119*, 1094−1100 (b) Deng, L.; Woo, T. K.; Cavallo, L.; Margl, P. M.; Ziegler, T. *J. Am. Chem. Soc.* **1997**, *119*, 6177−6186.

Scheme 4. 2 Formation of Alkyl Agostic Species via Multiple C_2H_4 Insertions from **1c**−**3c**

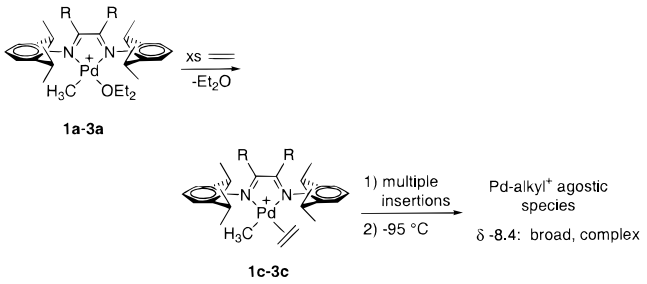

Scheme 5. Single Insertion of Ethylene To Give β-Agostic Isopropyl Complex **i-16**

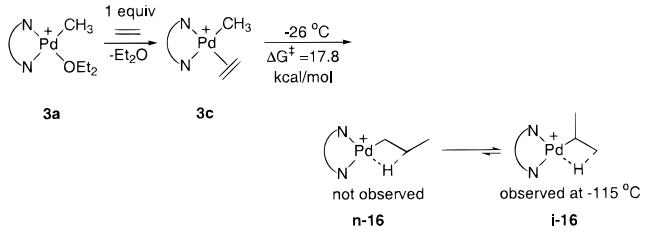

palladium catalysts indicates that the catalysts incorporate branches that contain branches.[27,29,68]

Well-defined Pd−alkyl species derived from **1c**−**3c** have been studied using variable temperature NMR spectroscopy to specifically probe factors contributing to the formation of polymer branches. Complexes **1c**−**3c** insert ethylene to yield a mixture of branched products after several turnovers, and the displaced ether does not recoordinate upon complete consumption of added olefin. The resulting ^{1}H NMR spectra at ca. −95 °C are relatively complex and contain a group of broad shifts at ca. −8.4 ppm that are consistent with the formation of alkyl agostic species (Scheme 4). Complexes arising from a single insertion of olefin into the Pd−CH_3 bond of **3c** exhibit relatively simple NMR spectra and are therefore ideally suited as models for polymerization intermediates. In particular, the acenaphthyl backbone of the ligand contains hydrogens that exhibit unique, resolved ^{1}H NMR shifts that simplify observation and characterization of reaction intermediates. These experiments are described below.

***β*-Agostic Isopropyl Complex.** Addition of a single equivalent of ethylene to an NMR tube containing **3a** dissolved in $CDCl_2F$ leads to displacement of coordinated ether by ethylene. Migratory insertion of the resulting methyl ethylene complex **3c** takes place at temperatures above −30 °C ($\Delta G^{\ddagger} = 17.8$ kcal/mol) to give a single species that displays dynamic behavior. The static ^{1}H and ^{13}C NMR spectra of this dynamic species can be observed at temperatures below ca. −110 °C. These static spectra are consistent with a β-agostic isopropyl complex, **i-16**, which presumably forms via rapid isomerization of the initial Pd−*n*-propyl insertion product, **n-16** (Scheme 5). The signal for the agostic hydrogen appears as a broad triplet at −8.0 ppm in the ^{1}H NMR spectrum with a geminal coupling constant of 17 Hz. The carbon of the agostic methyl group appears in the ^{13}C NMR spectrum at 19.5 ppm with $J_{CH} = 152$ and 65 Hz. The ether-free salt of **i-16** is fairly stable and can be prepared on a large scale and stored at −30 °C for extended periods without decomposition.[48]

The stability of the secondary isopropyl agostic complex relative to the primary *n*-propyl agostic complex was not expected on the basis of analogy to the normal stability order (1° > 2° > 3°) of metal alkyl complexes (presumed to be a steric effect). However, the inductive electron-donating ability of a secondary alkyl group is greater than that of a primary alkyl group and should provide more electron density to the electrophilic Pd metal center. Theoretical calculations have been reported for β-agostic *n*-propyl and isopropyl Pd−α-diimine compounds that predict a β-agostic isopropyl species to be favored by as little as 0.5 kcal/mol or by as much as 2.0 kcal/mol.[57] Although we have not directly observed **n-16** by NMR spectroscopy, ΔG for the **i-16/n-16** equilibrium was determined to be ca. 1.2−1.3 kcal/mol based on trapping experiments using dimethyl sulfide (vide infra).

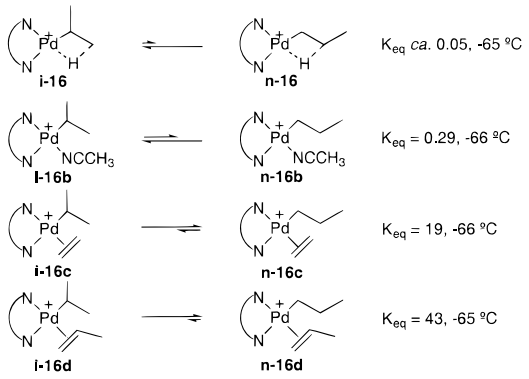

Figure 5. Equilibrium constants for trapped propyl isomers.

Isomerization of Cationic Pd−Alkyl Complexes. Various trapping ligands have been used to observe Lewis base adducts of **i-16** and **n-16**, yielding insight into the mechanism of chain-running.[69] Addition of 2 equiv of acetonitrile to an NMR sample of **i-16/n-16** at −78 °C gives almost exclusively the isopropyl acetonitrile complex **i-16b** by ^{1}H NMR spectroscopy. Isomerization to the *n*-propyl acetontrile complex **n-16b** begins to occur at temperatures above −70 °C, and an equilibrium value of 0.29 is observed for **n-16b/i-16b** at −66 °C. Use of ethylene as the trapping ligand under the same conditions results in initial trapping as **i-16c** with isomerization to **n-16c** again occurring above −70 °C. At −66 °C the *n*-propyl ethylene complex is favored with $K_{eq} = 19$ for **n-16c/i-16c**. In contrast to acetonitrile and ethylene, the ^{1}H NMR spectra indicate that addition of propylene to **i-16/n-16** at −78 °C yields predominantly the *n*-propyl propylene complex, **n-16d**, with $K_{eq} = 43$ at −65 °C for **n-16d/i-16d**. However, addition of 2 equiv of propylene at −130 °C allowed trapping of **i-16** as **i-16d**, with **i-16d** readily isomerizing to **n-16d** at temperatures above ca. −85 °C. Consideration of the equilibrium values shown in Figure 5 indicates that formation of the sterically less congested *n*-propyl complex becomes more favored with bulkier trapping ligands.

Isomerization of the isopropyl ethylene complex **i-16c** to the *n*-propyl ethylene complex **n-16c** models the chain-running process (eq 11). Several possible mechanisms may apply to this

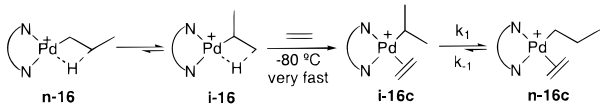

(11)

isomerization. One possibility is that isomerization occurs without ethylene loss, for example, through a five-coordinate

(68) Nelson, L. T. J.; McCord, E. F.; Johnson, L. K.; McLain, S. J.; Ittel, S. D.; Killian, C. M. *Polym. Prepr. (Am. Chem. Soc., Div. Polym. Chem.)* **1997**, *38(1)*, 133−134.

(69) For previous studies of alkyl isomerization in unhindered Pd systems, see: (a) Reger, D. L.; Garza, D. G.; Baxter, J. C. *Organometallics* **1990**, *9*, 873−874 (b) Reger, D. L.; Garza, D. G.; Lebioda, L. *Organometallics* **1991**, *10*, 902−906 (c) Reger, D. L.; Garza, D. G.; Lebioda, L. *Organometallics* **1992**, *11*, 4285−4292.

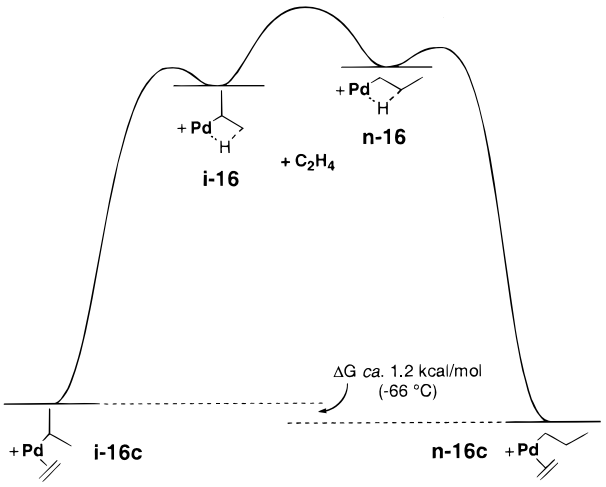

Figure 6. Free energy diagram for isomerization of **i-16c** according to Mechanism I.

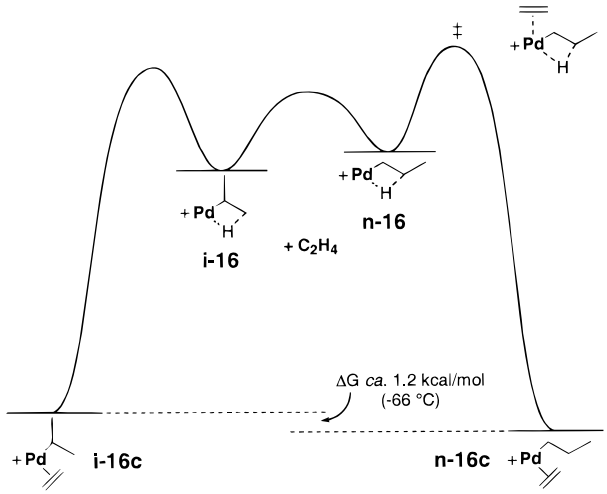

Figure 7. Free energy diagram for isomerization of **i-16c** according to Mechanism II.

bis-olefin hydride intermediate. Alternatively, isomerization may occur via ethylene loss, 1,2-migration of palladium in the alkyl cation, and recapture of ethylene. For the latter process, two limiting kinetic situations can apply and are illustrated as Mechanisms I and II in Scheme 6.

In Mechanism I, a rapid preequilibrium exists between **i-16c** and **i-16** + C_2H_4 (i.e., $k_{-1}[C_2H_4] > k_2$). The transition state for overall conversion of **i-16c** to **n-16c** lies between **i-16** and **n-16**. Kinetic analysis as shown in Scheme 6 indicates that if this mechanism pertains, the rate of isomerization of **i-16c** to **n-16c** should be inverse in ethylene and thus retarded by added ethylene. In Mechanism II the interconversion of alkyl cations **i-16** and **n-16** is rapid relative to the trapping reactions (i.e., k_2, $k_{-2} > k_{-1}[C_2H_4]$, $k_T[C_2H_4]$). The rapidly equilibrating cations **i-16** and **n-16** can, for kinetic analysis, be treated as a single species. As shown in Scheme 6, kinetic analysis of Mechanism II predicts *no* inhibition of the rate of conversion of **i-16c** to **n-16c** by added ethylene.

It is instructive to consider free energy diagrams for these two limiting mechanisms as shown in Figures 6 (Mechanism I) and 7 (Mechanism II). The key difference in these cases is that in Mechanism I the trapping barriers are much lower than the barrier to interconversion of the Pd−alkyl cations **i-16** and **n-16**, while in Mechanism II the trapping barriers are higher than the barriers to interconversion.

Table 3. Rate of Isomerization of **i-16c** to **n-16c**[a]

equiv of C_2H_4	k_1 ($\times 10^4$ s^{-1})	$\Delta G^{\ddagger}$ (kcal/mol)
1	2.9, −66 °C	15.3
5	2.8, −66 °C	15.3
10	2.5, −66 °C	15.4
45	1.8, −67 °C	15.4

[a] Error in $\Delta G^{\ddagger}$ values is ±0.1 kcal/mol.

Experiments were carried out in which the rate of isomerization of **i-16c** to **n-16c** was monitored as a function of added ethylene. Results are summarized in Table 3. Addition of 5 equiv of ethylene results in no measurable decrease in isomerization rate. Addition of 10 and 45 equiv of ethylene results in a small decrease in rate, but clearly the isomerization rate shows little dependence on the concentration of ethylene. These results suggest that either isomerization occurs from the four-coordinate

Scheme 6. Possible Mechanisms for Alkyl Isomerization

Mechanism I

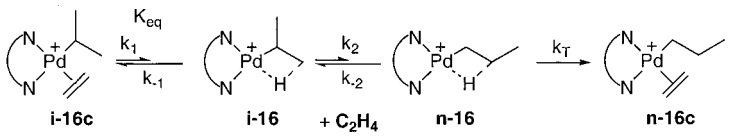

$$\frac{d(\textbf{n-16c})}{dt} = k_2(\textbf{i-16}) \qquad (\textbf{i-16}) = K_{eq}\frac{(\textbf{i-16c})}{(\textbf{C}_2\textbf{H}_4)} \qquad \boxed{\frac{d(\textbf{n-16c})}{dt} = k_2K_{eq}\frac{(\textbf{i-16c})}{(\textbf{C}_2\textbf{H}_4)}}$$

Mechanism II

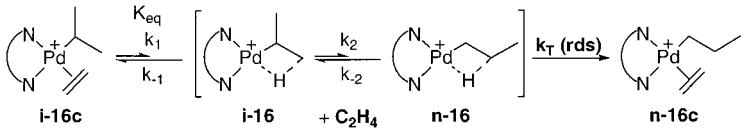

$$k_2,\ k_{-2} > k_{-1},\ k_T$$

$$\frac{d(\textbf{n-16c})}{dt} = k_T(\textbf{i-16} + \textbf{n-16})(\textbf{C}_2\textbf{H}_4) \qquad (\textbf{i-16} + \textbf{n-16}) = K_{eq}\frac{(\textbf{i-16c})}{(\textbf{C}_2\textbf{H}_4)}$$

$$\boxed{\frac{d(\textbf{n-16c})}{dt} = k_TK_{eq}(\textbf{i-16c})\frac{(\textbf{C}_2\textbf{H}_4)}{(\textbf{C}_2\textbf{H}_4)} = k_TK_{eq}(\textbf{i-16c})}$$

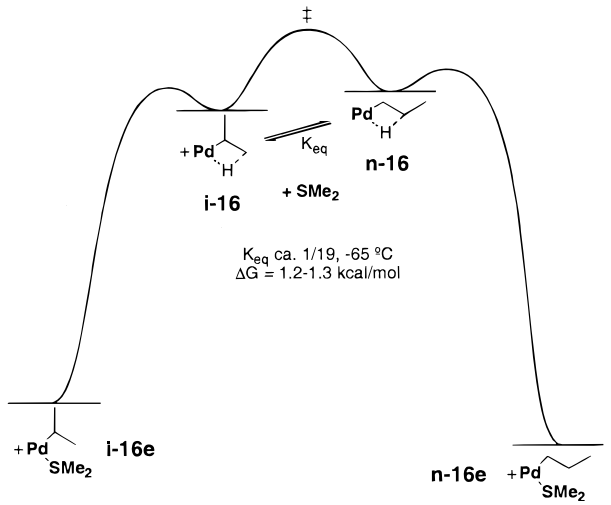

Figure 8. Free energy diagram for isomerization of **i-16e**.

resting state without ethylene loss or that Mechanism II applies in which the trapping barriers are higher than the interconversion barriers.

We reasoned that if Mechanism II applies in the case of ethylene, use of a small, much more nucleophilic trapping ligand would result in much lower barriers to trapping, and a limiting case, as described by Mechanism I, might be reached in which isomerization is now retarded by added trapping ligand. In contrast, if isomerization occurs without loss of trapping ligand then the rate should not be affected by additional ligand.

On the basis of previous equilibrium binding studies of ligands to Pd(II) centers, we chose to examine trapping and isomerization using dimethyl sulfide.[70] Addition of a single equivalent of Me_2S to **i-16/n-16** at −78 °C yields predominantly the isopropyl adduct **i-16e**, and subsequent isomerization to the *n*-propyl complex **n-16e** occurs only at temperatures above −50 °C (eq 12). Quantitative rate measurements were carried

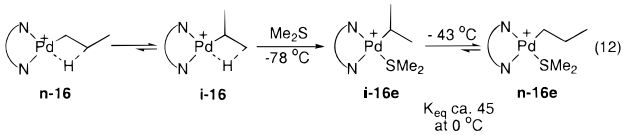

(12)

out at −43 °C. Addition of 1 equiv of Me_2S to **i-16/n-16** generates **i-16e** without free Me_2S present. Isomerization occurs by a clean first-order process with $k = 1.1 \times 10^{-4}$ s^{-1} at −43 °C. Addition of 5 equiv of Me_2S to **i-16/n-16** yields **i-16e** with 4 equiv of free Me_2S present. First-order isomerization to **n-16e** occurs at −43 °C with $k = 0.25 \times 10^{-4}$ s^{-1}. Clearly, free Me_2S greatly retards isomerization.

This result establishes that isomerization of **i-16e** occurs via Mechanism I and does not take place from **i-16e** without loss of Me_2S. The free energy diagram for the Me_2S case is shown in Figure 8. Since trapping below −50 °C is very fast relative to interconversion of **i-16** and **n-16**, the equilibrium ratio of **i-16:n-16** can be assessed by trapping at low temperature and carefully measuring the ratio of **i-16e**:**n-16e**. Table 4 summarizes K_{eq} values for **i-16/n-16** at three different temperatures together with the corresponding ΔG values, which are ca. 1.2−1.3 kcal/mol.

The results using dimethyl sulfide as the trapping ligand strongly suggest that in the case of ethylene, a weaker trapping ligand, Mechanism II applies. Reconsideration of the kinetic

(70) Rix, F. C.; Brookhart, M.; White, P. S. *J. Am. Chem. Soc.* **1996**, *118*, 4746−4764.

Table 4. Ground-State Energy Difference for **i-16** and **n-16**

temp (°C)	K_{eq} (**i-16/n-16**)	ΔG (kcal/mol)
−51.2	0.056	1.3
−65.2	0.053	1.2
−84.3	0.036	1.3

data in Table 3 suggests that the very small rate suppression observed at high free ethylene concentration is likely due to an increase in the rate of trapping to the point where trapping is becoming competitive with **i-16/n-16** interconversion. Under these conditions, the limiting kinetic analysis shown for Mechanism II will begin to break down and some rate retardation will be observed in this "intermediate" case.

Two additional features of these isomerizations should be noted. First, consistent with a mechanism involving loss of L for isomerization of [(N^N)Pd(*i*-Pr)(L)$^+$] to [(N^N)Pd(*n*-Pr)(L)$^+$], rates track the binding energies of the ligands[70] with the rate of L = $CH_3CH{=}CH_2$ > $CH_2{=}CH_2$ > CH_3CN > $(CH_3)_2S$. Second, the fact that ethylene exchange in palladium−methyl ethylene complexes occurs by an associative mechanism (vide infra) suggests that dissociation of ethylene (or other L) from [(N^N)Pd(Me)(L)$^+$] complexes may be highly disfavored. However, in contrast to the methyl complexes, [(N^N)Pd(propyl)(L)$^+$] complexes contain a β-hydrogen, and thus ligand dissociation may be greatly accelerated by an intramolecular displacement of L to form, in a concerted fashion, the β-agostic palladium−alkyl complexes **n-16** and **i-16**.

Rates of Interconversion of Agostic Species. Experiments conducted thus far suggest that interconversion of **i-16** and **n-16** is quite rapid, but no quantitative data are available to estimate these rates. Dynamic NMR experiments are described here which attempt to address this problem. The static ^{1}H NMR spectrum of β-agostic isopropyl complex **i-16** contains a resonance at 2.88 ppm corresponding to the methine hydrogen of the Pd−isopropyl group. Conversion of **i-16** to **n-16** and return could result in exchange of the methine hydrogen with the methyl hydrogen; thus line shape analysis of this shift could be useful for investigating interconversion of **i-16** and **n-16**. However, this shift is obscured by the isopropyl methine signals of the ligand. In fact, the methine signal could only be assigned at 2.88 ppm on the basis of a COSY experiment performed at ca. −110 °C.[48] To circumvent this problem, complex **6a** was employed in the synthesis of a β-agostic isopropyl analogue **i-17** bearing methyl rather than isopropyl substituents in the ortho positions of the ligand aryl rings (eq 13).

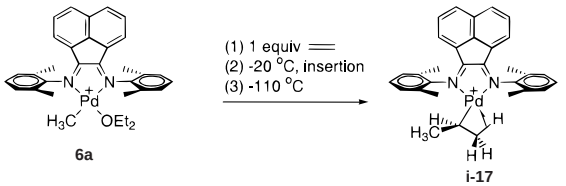

(13)

The methine hydrogen of the Pd−isopropyl group of **i-17** resonates as a septet at 2.9 ppm and begins to display line broadening at ca. −65 °C. Broadening results from exchange of the methine hydrogen (H′) with a hydrogen from one of the isopropyl methyl groups (i.e., **i-17** → **i-17′**, Scheme 7). This occurs via β-hydride elimination from **i-17** and reinsertion to give **n-17**, followed by rotation about the $C_\alpha-C_\beta$ bond of **n-17** to give **n-17′**, and finally β-hydride elimination/reinsertion to give **i-17′**.

Approximate rate constants for this exchange ($k_{H'}$) were determined by line-shape analysis (Table 5). If the barrier to rotation leading to agostic exchange (**n-17** → **n-17′**: $\Delta G_{rot}^{\ddagger}$) is

Scheme 7. Methine (H′) Exchange in β-Agostic Isopropyl Complex **i-17**

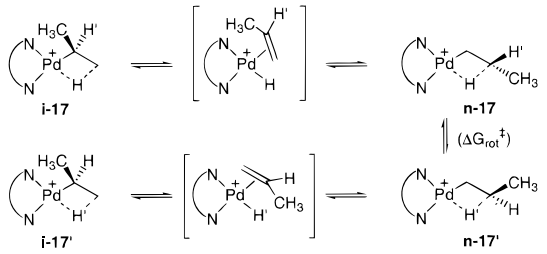

Table 5. Kinetic Data from Exchange of the Methine Hydrogen of **i-17**[a]

T (°C)	$\Delta W_{1/2}$ (Hz)[b]	$k_{H'}$ (s^{-1})[c]	$\Delta G_{H'}^{\ddagger}$ (kcal/mol)	k_{conv} (s^{-1})	$\Delta G_{conv}^{\ddagger}$ (kcal/mol)
−55	11	35	11.1	70	10.7
−45	37	115	11.1	230	10.7

[a] Error in $\Delta G^{\ddagger}$ is ±0.1 kcal/mol. [b] Change in width at half-height relative to the static spectrum at −110 °C. [c] From slow exchange approximation, $k = \pi\Delta\nu$.

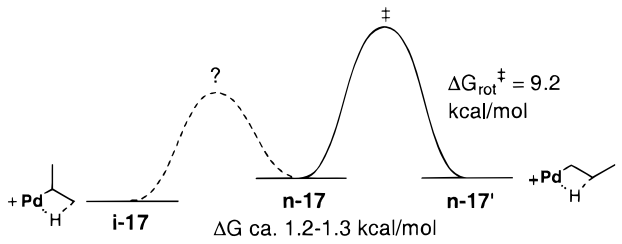

Figure 9. Free energy diagram for interconversion of **i-17** and **n-17**.

assumed to be low relative to β-hydride elimination and reinsertion (**i-17** → **n-17**), $k_{H'}$ will be equal to one-half the rate constant for conversion of **i-17** to **n-17** (since half the time **n-17**/**n-17′** could return with no site exchange of H′). A barrier for conversion ($\Delta G_{conv}^{\ddagger}$) of 10.7 kcal/mol can be calculated in this case by simply doubling $k_{H'}$ (Table 5). However, the assumption of a low **n-17**→**n-17′** (and **n-17′** → **n-17**) barrier relative to **i-17** → **n-17** conversion may be incorrect. A value of 9.2 kcal/mol can be estimated for $\Delta G_{rot}^{\ddagger}$ based on results obtained using **i-16**,[48] and ΔG for **n-17**/**i-17** can be estimated at 1.2−1.3 kcal/mol from results previously described here.

As shown in Figure 9, assuming the barrier to conversion of **i-17** to **n-17** to be *less* than **n-17** to **n-17′**, the predicted barrier for conversion of **i-17** to **i-17′** is $\Delta G + \Delta G_{rot}^{\ddagger} = 1.3$ kcal/mol + 9.2 kcal/mol = 10.5 kcal/mol, which is quite close to the observed barrier of 10.7 kcal/mol. Thus, based on this analysis, the magnitude of the **i-17** to **n-17** barrier is not certain. This barrier cannot be greater than 10.7 kcal/mol but may in fact be substantially less. If the barrier is significantly less than 10.7 kcal/mol, this implies that a 1,2-migration of Pd between the α and β carbons in a β-agostic alkyl complex is much more facile than migration to the carbons adjacent to C_α and C_β.

The process of interconversion between β-agostic *n*-propyl and β-agostic isopropyl−palladium species has been modeled by Morokuma, et al. (Figure 10).[56,57] As previously mentioned, the energy difference between the two agostic intermediates is predicted to be ca. 0.5 kcal/mol. The barrier to β-hydride elimination from each agostic intermediate is reported to be only 0.2-0.8 kcal/mol above the energy of the resulting propylene hydride species.[56] β-Hydride elimination from the isopropyl species of an unsubstituted model is predicted to give an olefin hydride species that is 7.4 kcal/mol higher in energy, so the barrier to this process can be estimated to be less than 8.2 kcal/

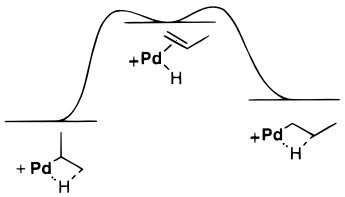

Figure 10. Modeled interconversion of β-agostic species through a propylene hydride intermediate.[56,57]

Scheme 8. Associative Ethylene Exchange

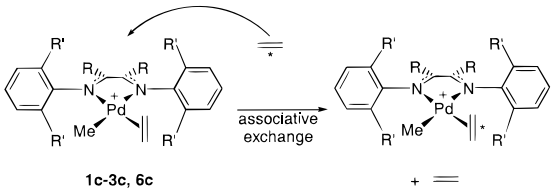

Table 6. Rate Constants for Ethylene Exchange

complex	rate constant (M^{-1} s^{-1})
1c (R = H, R′ = *i*-Pr)	8200
2c (R = CH_3, R′ = *i*-Pr)	45
3c (R,R = An, R′ = *i*-Pr)	560
6c (R,R = An, R′ = Me)	2600

mol. Using a more sterically encumbered model, an energy difference between the β-agostic isopropyl intermediate and the propylene−hydride complex is reported to be only 0.7 kcal/mol, indicating that rearrangement should be incredibly facile. Although the predicted energy barriers to β-hydride elimination for both model systems are significantly different from one another, these results suggest that the overall barrier to interconversion between **i-17**/**n-17** above may be substantially less than the upper limit of 10.7 kcal/mol determined by line-shape analysis.

Chain Transfer. Slow rates of chain transfer relative to propagation distinguish these Pd- and Ni-based α-diimine systems from most other late metal catalysts (Scheme 1B). Chain transfer may occur by exchange of bound olefinic polymer with free ethylene from an olefin hydride species (Scheme 1B(i)). Alternatively, Ziegler et al. have suggested based on DFT calculations that chain transfer occurs by concerted β-hydride transfer from the growing polymer chain to bound ethylene.[51,52] Subsequent exchange of the unsaturated polymer with ethylene must then occur from an *alkyl* olefin intermediate rather than from an olefin hydride species (Scheme 1B(ii)).

To assess the influence of steric bulk on the associative displacement of ethylene from the coordination sphere of these complexes (as in the proposed chain transfer mechanism shown in Scheme 1B(i)), the rate of exchange of bound ethylene with free ethylene (Scheme 8) was monitored for ethylene complexes **1c**−**3c** and **6c** by ^{1}H NMR line-broadening experiments at −85 °C (Table 6, rate constants). Line widths (w) were measured at half-height in units of hertz for complexed ethylene and were corrected for line widths in the absence of exchange (w_o). The exchange rates were determined from the standard equation for the slow exchange approximation: $\pi(w - w_o)/[C_2H_4]$, where $[C_2H_4]$ is the concentration of free ethylene.

The exchange rate of bound ethylene is clearly proportional to the concentration of free ethylene, which indicates that exchange takes place through an associative mechanism. As the size of the ligand backbone substituents is increased, the ligand aryl rings are forced to a greater extent into the plane perpendicular to the square plane of the complex. This causes

2the isopropyl groups to block the axial coordination sites of the metal center more effectively. As coordination of a second equivalent of ethylene becomes less favored, the rate of exchange is observed to decrease in the order R = H > R,R = An > R = CH_3. This is in agreement with experiment where the M_n's of the polyethylenes made using the same three catalysts are observed to *increase* in the same order. The rate of exchange of ethylene also increases as the size of the substituents on the aryl rings decreases from isopropyl to methyl (complex **3c** to complex **6c** in Table 6), indicating the increased effectiveness of the isopropyl groups relative to methyl at blocking the axial coordination sites in these systems.

It is also significant to note that ethylene exchange in (phen)-$Pd(CH_3)(C_2H_4)^+$ is too fast to be measured by NMR techniques, even at −100 °C. These systems dimerize ethylene, indicating that the rate of chain transfer is much greater than propagation, consistent with the complete absence of axial bulk in these systems.

These observations are not only consistent with the associative exchange mechanism 1B(i), but they are also fully consistent with the Ziegler β-H transfer to monomer mechanism 1B(ii), since the transition state for this process effectively places two olefinic moieties in axial sites (see **14**‡, Scheme 1B(ii)).

Summary

Pd(II) and Ni(II) complexes of aryl-substituted α-diimines bearing bulky ortho substituents polymerize ethylene to high molecular weight, highly branched polyethylene and α-olefins to polymers with unique microstructures bearing fewer branches than expected. This initial discovery[18] was a significant advance in the development of late metal catalysts for olefin polymerization and has resulted in much increased activity in this area. The studies described here have exposed numerous mechanistic details concerning these Pd(II) catalysts. The key findings are as follows:

(1) The catalyst resting states are (N^N)Pd(R)(olefin)$^+$ complexes. Turnover frequencies are controlled by the rates of migratory insertions of these species, and thus the rate of chain growth is independent of olefin concentration.

(2) Increasing the bulk of the ortho substituents on the aryl groups (as well as on the backbone carbons) lowers the barrier to insertions and raises the TOF. Presumably this arises from greater relief of steric crowding in the transition state for insertion relative to the ground state for the bulkier substituents.

(3) The intermediates formed upon migratory insertion of (N^N)Pd(alkyl)(olefin)$^+$ complexes (catalyst resting states) are dynamic, β-agostic (N^N)Pd(R)$^+$ complexes.

(4) Branching in the polyethylene is a result of metal migration along the chain in the cationic β-agostic palladium−alkyl complexes via repetitive β-elimination/reinsertion sequences.

(5) Chain walking can occur in the palladium alkyl olefin resting states, but these species do not undergo β-hydride elimination/reinsertion reactions. Rather, the process involves (reversible) loss of ethylene to yield cationic β-agostic palladium−alkyl species which undergo facile β-elimination/reinsertion reactions. Judging from the model systems studied here, the difference in barriers to 1,2 chain isomerization in the resting state and migratory insertion are ca. 2.5−3.0 kcal/mol. Thus, an average of ca. 100 1,2-migrations occur at 25 °C prior to insertion. This clearly explains why polyethylene produced from palladium catalysts is so highly branched.

(6) The rate of associative ethylene exchange in (ArN^NAr)-$Pd(alkyl)(C_2H_4)^+$ complexes decreases with increasing bulk of ortho and backbone substituents. This observation is consistent with chain transfer occurring via associative exchange from a palladium olefin hydride intermediate as originally proposed, where the transition state places both incoming and outgoing olefins in axial positions. It is also consistent with β-hydrogen transfer to monomer in the resting state, since Ziegler's calculations suggest that the transition state for this process resembles a bis-olefin hydride with both olefins occupying axial positions.

(7) Decomposition of (ArN^NAr)$Pd(CH_3)(L)^+$ species can occur by C−H activation of ortho isopropyl and *tert*-butyl substituents after loss of L to generate CH_4 and metallacycles. It is not clear whether such decomposition pathways are responsible for catalyst decay.

Experimental Section

General Considerations. All manipulations of compounds were performed using standard high-vacuum, Schlenk, or drybox techniques. Argon was purified by passage through columns of BASF R3-11 catalyst (Chemalog) and 4 Å molecular sieves. ^{1}H and ^{13}C NMR chemical shifts were referenced to residual ^{1}H NMR signals and to the ^{13}C NMR signals of the deuterated solvents, respectively, unless otherwise noted. NMR probe temperatures were measured using an external anhydrous methanol sample. All coupling constants are reported in hertz. Elemental analyses were performed by Atlantic Microlab Inc. of Norcross, GA, or by Oneida Research Services of Whitesboro, NY.

Materials. All solvents were deoxygenated and dried via passage over a column of activated alumina.[71] Dichlorofluoromethane-*d* ($CDCl_2F$) was prepared according to the literature.[72] Dichlorofluoromethane-*d* and methylene chloride-d_2 were dried over CaH_2 or P_2O_5, degassed by repeated freeze−pump−thaw cycles, vacuum-transferred, and stored over 4 Å molecular sieves. Polymer grade ethylene and CP grade propylene were used without further purification for preparative scale polymerizations and NMR experiments. The α-diimine ligands (except for 2-C_6H_4(*t*-Bu)N=C(R)C(R)=N-2-C_6H_4(*t*-Bu), R = Me and R,R = An) were prepared according to the literature,[50,58−60] and (2,6-C_6H_4(*i*-Pr)$_2$−N=C(R)C(R)=N-2,6-C_6H_4(*i*-Pr)$_2$)$PdMe_2$[50] has previously been prepared and characterized. Our group has earlier reported the preparation of dimethyl complexes (2,6-C_6H_4(*i*-Pr)$_2$N=C(R)C(R)=N-2,6-C_6H_4(*i*-Pr)$_2$)$PdMe_2$ (R = H and R = Me), and their ether complexes **1a** and **2a**.[18] In addition, characterization of the ethylene, propylene, and butene adducts of **1a** and **2a** and details of the resulting insertion products were reported in the Supporting Information of this same reference.[18] (COD)PdMeCl (COD = 1,5-cyclooctadiene),[61] (COD)-$PdMe_2$,[62] (pyridazine)$PdMe_2$,[64] $NaBAr'_4$,[73,74] and $H(OEt_2)_2BAr'_4$ (Ar′ = 3,5-$C_6H_3(CF_3)_2$)[75,76] were prepared as described in the literature.

Synthesis of Ligands. (a) 2-C_6H_4(*t*-Bu)N=C(Me)C(Me)=N-2-C_6H_4(*t*-Bu). A flask was charged with 2-*tert*-butylaniline (5.00 mL, 32.1 mmol) and 2,3-butanedione (1.35 mL, 15.4 mmol). Addition of 10 mL of methanol and ca. 1 mL of formic acid gave formation of a yellow precipitate within 30 s. A yellow solid was collected by filtration after stirring for 19 h. This solid was dissolved in diethyl ether, and the solution was stirred over Na_2SO_4, filtered, condensed, and placed into a −30 °C freezer for crystallization. Large, bright yellow crystals were collected via filtration and dried under vacuum. After isolating a second crop of crystals, an overall yield of 86% (4.6 g) was obtained. ^{1}H NMR ($CDCl_3$, 300 MHz) δ 7.43 (dd, 2H, J = 7.85, 1.33 Hz), 7.20 (ddd, 2H, J = 7.4, 7.2, 1.4 Hz), 7.09 (ddd, 2H, J = 7.6, 7.6, 1.4 Hz),

(71) Pangborn, A. B.; Giardello, M. A.; Grubbs, R. H.; Rosen, R. K.; Timmers, F. J. *Organometallics* **1996**, *15*, 1518−1520.

(72) Siegel, J. S.; Anet, F. A. L. *J. Org. Chem.* **1988**, *53*, 2629−2630.

(73) Nishida, H.; Takada, N.; Yoshimura, M.; Sonoda, T.; Kobayashi, H. *Bull. Chem. Soc. Jpn.* **1984**, *57*, 2600−2604.

(74) Caution: Preparation of the Grignard reagent from 3,5-$(CF_3)_2C_6H_3$-Br can result in explosions. This material is commercially available from Boulder Scientific.

(75) Brookhart, M.; Grant, B.; Volpe Jr., A. F. *Organometallics* **1992**, *11*, 3920−3922.

(76) The chemical shift originally reported for the oxonium proton in $H(OEt_2)_2BAr'_4$ (δ 11.1) is incorrect; this peak is caused by the presence of H_2O in the sample. The correct chemical shift is δ 16.7 (9 peaks, J = 1.5 Hz, 1H).

6.52 (dd, 2H, J = 7.7, 1.4 Hz), 2.22 (s, 6H), 1.36 (s, 18H). $^{13}C\{^1H\}$ NMR ($CDCl_3$, 75 MHz) δ 167.0, 149.5, 139.6, 126.62, 126.58, 124.2, 119.5, 35.32, 29.7, 16.62. Anal. Calcd for $C_{24}H_{32}N_2$: C, 82.71; H, 9.25; N, 8.04. Found: C, 82.69; H, 9.21; N, 8.01.

(b) 2-C_6H_4(*t*-Bu)N═C(An)C(An)═N-2-C_6H_4(*t*-Bu). A flask was charged with 2-*tert*-butylaniline (3.00 mL, 19.2 mmol) and acenaphthenequinone (1.71 g, 9.39 mmol). The reagents were partially dissolved in 50 mL of methanol (acenaphthenequinone was not completely soluble), and formic acid (1−2 mL) was added. An orange solid formed and was collected via filtration after stirring for 19 h. This solid was dissolved in CH_2Cl_2, the solution was stirred over Na_2SO_4 and filtered, and the product reprecipitated upon cooling (3.51 g, 84.1%). ^1H NMR ($CDCl_3$, 300 MHz) δ 7.85 (d, 2H, J = 8.2 Hz, An: H_p), 7.59 (m, 2H, Ar: H_m), 7.37 (dd, 2H, J = 7.8, 7.6 Hz, An: H_m), 7.27 (m, 4H, Ar: H_m and H_p), 7.01 (m, 2H, Ar: H_o), 6.91 (d, 2H, J = 7.2 Hz, An: H_o), 1.46 (s, 18H, C(CH_3)$_3$). $^{13}C\{^1H\}$ NMR ($CDCl_3$, 75 MHz) δ 159.9, 150.6, 141.8, 139.3, 131.2, 129.1, 128.8, 127.7, 126.83, 126.75, 124.6, 123.9, 119.0, 35.5, 29.8. Anal. Calcd for $C_{32}H_{32}N_2$: C, 86.45; H, 7.25; N, 6.30. Found: C, 86.31; H, 7.29; N, 6.22.

Synthesis of Dimethyl Complexes. (a) (ArN═C(An)C(An)═NAr)-Pd(CH_3)$_2$ (Ar = 2,6-C_6H_3(*i*-Pr)$_2$). A Schlenk flask was charged with 0.2658 g (1.003 mmol) of (COD)PdMeCl and cooled to −30 °C. Ether (25 mL) was added via syringe followed by MeLi (0.75 mL of a 1.6 M solution in ether, ca. 1.2 equiv), and the mixture was stirred with warming to −10 °C. At this stage white LiCl had precipitated out and *tert*-butyl bromide (0.05 mL, 0.43 mmol) was added to consume any excess MeLi. The ligand, 2,6-C_6H_3(*i*-Pr)$_2$N═C(An)C(An)═N-2,6-C_6H_3(*i*-Pr)$_2$ (0.5051 g, 1.002 mmol), was added as a cooled (−10 °C) slurry in 25 mL of diethyl ether, and the resulting mixture was stirred for about 1 h as the flask warmed to 25 °C. The product was transferred to another flask using ca. 125 mL of Et_2O, the solvent was removed under vacuum, and the residue was washed with pentane until the washes were colorless (5 × 10 mL). The solid was dried overnight in vacuo to give 0.289 g (0.454 mmol) of a green powder (45.3% yield). The ^1H and ^{13}C NMR spectroscopic data for this compound have been reported.[60] Anal. Calcd for $C_{38}H_{46}N_2Pd$: C, 71.63; H, 7.28; N, 4.40. Found: C, 71.60; H, 7.24; N, 4.48.

(b) (ArN═C(An)C(An)═NAr)Pd(CH_3)$_2$ (Ar = 2-C_6H_4(*t*-Bu)). A Schlenk flask was charged with 0.097 g (0.396 mmol) of (COD)PdMe_2 in a glovebox equipped with a −30 °C freezer, taking precautions to keep the precursor and glassware as cold as possible at all times. The flask was brought out of the glovebox and rapidly cooled to −40 °C in a dry ice/2-propanol bath. The solid was dissolved in 15 mL of ether, and the diimine 2-C_6H_4(*t*-Bu)N═C(An)C(An)═N-2-C_6H_4(*t*-Bu) (0.178 g, 0.400 mmol) was cannulated onto the stirring solution as a slurry in 25 mL of ether. The reaction was warmed to 0 °C, and stirring was continued for approximately 2 h. The reaction flask was stored at −30 °C overnight, resulting in formation of a green precipitate which was isolated via filtration and dried in vacuo. A second green solid resembling the first was collected upon evaporation of solvent under vacuum from the supernatant. The solids were combined, washed with hexanes (2 × 10 mL), and dried in vacuo to yield 0.197 g (85.6%) of the desired product (two isomers, presumbly from cis and trans ligand conformations, in a ratio of ca. 97:3). ^1H NMR (CD_2Cl_2, 300 MHz) major: δ 8.01 (d, 2H, J = 8.3 Hz, An: H_p), 7.66 (m, 2H, H_{aryl}), 7.43−7.34 (m, 6H, An: H_m, 2H_{aryl}), 7.05 (m, 2H, H_{aryl}), 6.54 (d, 2H, J = 7.5 Hz, An: H_o), 1.45 (s, 18H, C(CH_3)$_3$), −0.05 (s, 6H, PdMe_2); minor: δ 7.90 (d, 2H, J = 8.3 Hz), 7.56 (m, 2H), obscured (2H_{aryl}), 7.25 (m, 4H), 6.93 (m, 2H), 6.85 (d, 2H, J = 7.1 Hz), 1.37 (s, 18H), obscured (6H, PdMe_2). $^{13}C\{^1H\}$ NMR (CD_2Cl_2, 75 MHz) δ 167.7 (N═*C*−*C*−N), 147.2 (Ar: C_{ipso}), 143.7, 131.6 (An: 2 quaternary C), 140.6 (N═C(*C*)−C(*C*)═N), 128.24 (Ar: *C*−C(CH_3)$_3$), 130.22, 128.84, 128.43, 127.52, 126.68, 125.23, 122.49, 36.3 (*C*(CH_3)$_3$, 31.5 (*C*(CH_3)$_3$, −6.29 (Pd*Me*, J_{CH} = 128.1 Hz) (minor isomer not detected). Anal. Calcd for $C_{34}H_{38}N_2Pd$: C, 70.27; H, 6.59; N, 4.82. Found: C, 69.98; H, 6.87; N, 4.69.

(c) (ArN═C(An)C(An)═NAr)Pd(CH_3)$_2$ (Ar = 2,6-C_6H_3(Me)$_2$). A Schlenk flask was charged with 0.4150 g (1.916 mmol) of [(pyridazine)-Pd(CH_3)$_2$]$_n$ and 0.7520 g of ArN═C(An)C(An)═NAr (1.936 mmol). The flask was cooled to 0 °C, 50 mL of diethyl ether was added via syringe, and the mixture was stirred at 0 °C for 2 h and at room temperature for 1 h. The ether solution was filtered into another Schlenk flask, and the remaining product was extracted with CH_2Cl_2, leaving behind a significant amount of Pd(0). The solvents were removed under vacuum, and the residue was washed with pentane until the washes were colorless (5 × 20 mL). Recrystallization from ether layered with pentane (ca. 2:1), filtration, and drying in vacuo gave 0.376 g (0.717 mmol) of green microcrystals (two crops, 37.4% yield). ^1H NMR ($CDCl_3$, 300 MHz) δ 8.00 (d, 2H, J = 8.4 Hz, An: H_p), 7.41 (dd, 2H, J = 8.3, 7.2 Hz, An: H_m), 7.23−7.19 (m, 6H, 6 H_{aryl}), 6.71 (d, 2H, J = 7.2 Hz, An: H_o), 2.29 (s, 12H, 2,6-C_6H_3(*Me*)$_2$), 0.02 (s, 3H, PdMe_2). Anal. Calcd for $C_{30}H_{30}N_2Pd$: C, 68.63; H, 5.76; N, 5.34. Found: C, 68.64; H, 5.82; N, 5.32.

Synthesis of Catalysts. (a) Spectral Data for the BAr′$_4$ Counterion. The ^1H and ^{13}C NMR resonances of the [B{3,5-C_6H_3(CF_3)$_2$}$_4$]$^-$ anion in CD_2Cl_2 were essentially invariant for different complexes, and temperatures and are not repeated in all of the spectroscopic data for each of the cationic complexes: ^1H NMR (CD_2Cl_2) δ 7.7 (s, 8, H_o), 7.5 (s, 4, H_p); $^{13}C\{^1H\}$ NMR (CD_2Cl_2) δ 162.2 (q, $^1J_{CB}$ = 49.8, C_{ipso}), 135.2 (C_o), 129.3 (q, $^2J_{CF}$ = 31.7, C_m), 125.0 (q, $^1J_{CF}$ = 272.5, CF_3), 117.9 (C_p).

(b) [(ArN═C(An)C(An)═NAr)Pd(CH_3)(OEt$_2$)]BAr′$_4$ (Ar = 2,6-C_6H_3(*i*-Pr)$_2$), 3a. A Schlenk flask was charged with 0.195 g (0.306 mmol) of (2,6-C_6H_3(*i*-Pr)$_2$N═C(An)C(An)═N-2,6-C_6H_3(*i*-Pr)$_2$)Pd(CH_3)$_2$ and 0.309 g (0.305 mmol) of H(OEt$_2$)$_2$BAr′$_4$. The flask was cooled to −78 °C, and 10 mL of ether were added via syringe. The stirring suspension was warmed to 0 °C in an ice bath, resulting in formation of a dark red solution. The solution was filtered, and the ether was removed under vacuum to give an orange powder which was further dried in vacuo, yielding 0.425 g of product (89% yield). ^1H NMR (CD_2Cl_2, −30 °C, 300 MHz): δ 8.08 (d, 1H, J = 8.4 Hz, An: H_p), 8.04 (d, 1H, J = 8.4 Hz, An: $H_{p'}$), 7.36−7.34 (m, 8H, An: H_m, H_m′; 6 H_{aryl}), 6.64 (d, 1H, J = 7.3 Hz, An: H_o), 6.37 (d, 1H, J = 7.3 Hz, An: H_o′), 3.36 (q, 4H, J = 7.0 Hz, O(CH_2CH$_3$)$_2$), 3.16 (2 septets, 2H each, J = 6.8 Hz, C*H*Me$_2$, C′*H*Me$_2$), 1.35 (d, 6H, J = 6.9 Hz, CH*Me*Me′), 1.32 (d, 6H, J = 6.9 Hz, CHMe*Me*′), 1.26 (t, 6H, J = 6.9 Hz, O(CH$_2$CH_3)$_2$), 0.86 (2d, 6H each, J = 6.5 Hz, C′H*MeMe*′), 0.67 (s, 3H, Pd*Me*). $^{13}C\{^1H\}$ NMR (CD_2Cl_2, −30 °C, 75 MHz): δ 174.5 and 168.6 (N═*C*−*C*′═N), 140.9 and 139.4 (Ar, Ar′: C_{ipso}), 138.2 and 137.1 (Ar, Ar′: C_o), 144.7, 132.5, 131.8, 130.5, 129.2, 128.7, 128.2, 128.0, 127.8, 125.4, 125.2, 124.9, 124.6, and 124.4 (An: 4 quaternary C; An: C_o,C_o′, C_p, C_p′, C_m, C_m′; Ar, Ar′: C_m, C_p), 71.7 (O(*C*H$_2$CH$_3$)$_2$), 28.7 and 28.4 (*C*HMe$_2$, *C*′HMe$_2$), 23.86, 23.56, 22.59, and 22.45 (CH*MeMe*′, C′H*MeMe*′), 14.7 (O(CH$_2$*C*H$_3$)$_2$), 9.6 (Pd*Me*). Anal. Calcd for $C_{73}H_{65}N_2BF_{24}OPd$: C, 56.22; H, 4.20; N, 1.80. Found: C, 56.46; H, 4.14; N, 1.82.

(c) [(ArN═C(An)C(An)═NAr)Pd(CH_3)(OEt$_2$)]BAr′$_4$ (Ar = 2-C_6H_4-(*t*-Bu)), 5a. This compound was synthesized using a procedure identical to that described above for **3a**. The dimethyl complex, 2-C_6H_4(*t*-Bu)N═C(An)C(An)═N-2-C_6H_4(*t*-Bu))Pd(CH_3)$_2$ (0.106 g, 0.182 mmol), and H(OEt$_2$)$_2$BAr′$_4$ (0.185 g, 0.183 mmol) were combined in a Schlenk flask. Ether (5 mL) was added, and the reaction was warmed to 0 °C. Isolation via removal of the solvent under vacuum yielded 0.260 g of a dark red solid (0.173 mmol, 94.8%). Importantly, only a single isomer is observed by NMR spectroscopy. Each of several attempts at preparing this compound was accompanied by 5−15% intramolecular C−H activation to give the six-membered palladacycle. ^1H NMR (CD_2Cl_2, −80 °C, 300 MHz) δ 8.09 (d, 1H, J = 9.0 Hz, An: H_p), 8.06 (d, 1H, J = 9.3 Hz, An: $H_{p'}$), 7.72−7.32 (m, 8H, An: H_m, H_m′; 6 H_{aryl}), 7.04 (dd, 2H, J = 7.2, 7.2 Hz, 2 H_{aryl}), 6.54 (d, 1H, J = 7.5 Hz, An: H_o), 6.24 (d, 1H, J = 7.5 Hz, An: H_o′), 3.37 (q, 4H, J = 6.9 Hz, O(*C*H$_2$CH$_3$)$_2$), 1.43 (s, 9H, C(*C*H$_3$)$_3$), 1.38 (s, 9H, C′(*C*H$_3$)$_3$), 1.09 (t, 6H, J = 6.9 Hz, O(CH$_2$*C*H$_3$)$_2$), 0.80 (s, 3H, P,*Me*).

(d) [(ArN═C(An)C(An)═NAr)Pd(CH_3)(OEt$_2$)]BAr′$_4$ (Ar = 2,6-C_6H_3(Me)$_2$), 6a. Following the above procedure for protonation described for catalysts **3a** and **5a** in this case yielded a clean mixture of two products that could not be separated (ca. 4:1 desired/side product). The side product was not clearly identified but may consist of a methyl-bridged dimeric monocation. A second attempt was made under slightly modified conditions. A Schlenk flask was charged with 0.578 g (0.571 mmol) of H(OEt$_2$)$_2$BAr′$_4$ and cooled to −78 °C and 8 mL of ether was added via syringe. The flask was carefully warmed

just until the acid was dissolved. A second flask, charged with a suspension of 0.300 g (0.571 mmol) of (2,6-$C_6H_3(Me)_2$N=C(An)C(An)=N-2,6-$C_6H_3(Me)_2$)Pd(CH_3)$_2$ in 10 mL of ether, was also cooled to −78 °C. Most of this suspension was transferred via cannula into the flask containing the dissolved acid. Additional ether (4 mL) was added to the residual dimethyl complex; this suspension was cooled and added as well. The reaction mixture became a bright orange/red solution with a small amount of dark solid after stirring at −78 °C for ca. 15 min. The solution was rapidly filtered into another cooled Schlenk flask (−78 °C), and the solvent was removed under reduced pressure to give 0.635 g (0.439 mmol) of a light orange powder (76.5% yield). ^{1}H NMR (CD_2Cl_2, −80 °C, 300 MHz) δ 8.09 (d, 1H, J = 9.0 Hz, An: H_p), 8.05 (d, 1H, J = 9.3 Hz, An: H_p'), 7.46−7.17 (m, 8H, An: H_m, H_m'; 6 H_{aryl}), 6.67 (d, 1H, J = 7.5 Hz, An: H_o), 6.39 (d, 1H, J = 7.5 Hz, An: H_o'), 2.23 (q, 4H, J = 6.3 Hz, O(CH_2CH_3)$_2$), 2.23 and 2.19 (2 s, 6H each, 2,6-$C_6H_3(Me)_2$ and 2,6-$C_6H_3(Me')_2$), 1.48 (t, 6H, J = 1.5 Hz), O(CH_2CH_3)$_2$), 0.53 (s, 3H, Pd*Me*). ^{13}C{^{1}H} NMR (CD_2Cl_2, −80 °C, 300 MHz) δ 174.4 and 168.5 (N=*C*−*C*′=N), 144.9, 143.2 (Ar, Ar′: C_{ipso}), 141.9 (2 C, Ar, Ar′: C_o), 132.6, 132.0, 130.2, 129.1, 128.9, 128.1, 127.9, 127.2, 126.7, 126.6, 124.9, 124.7, 124.6, 124.3, 71.8 (O(*C*H_2CH$_3$)$_2$), 17.5 and 17.3 (2,6-$C_6H_3(Me)_2$, 2,6-$C_6H_3(Me')_2$), 16.4 (O(CH_2CH_3)$_2$), 9.5 (Pd*Me*). Anal. Calcd for $C_{65}H_{49}N_2BF_{24}$OPd: C, 53.94; H, 3.41; N, 1.94. Found: C, 54.22; H, 3.46; N, 2.05.

(e) [(ArN=C(Me)C(Me)=NAr)Pd(CH_3)(NCMe)]BAr′$_4$ (Ar = 2-C_6H_4(*t*-Bu)), 4b. A Schlenk flask was charged with 0.180 g (0.679 mmol) of (COD)PdMeCl and 0.602 g (0.679 mmol) of NaBAr′$_4$. After cooling the flask to −40 °C, 25 mL of CH_2Cl_2 and 25 mL of NCMe were added by syringe. The reaction was stirred with warming to −20 °C, resulting in formation of [(COD)Pd(Me)(NCMe)]BAr′$_4$ accompanied by precipitation of NaCl. After allowing the precipitate to settle, the solution of NCMe adduct was cannula filtered into another Schlenk flask cooled to 0 °C and containing a suspension of 0.237 g (0.679 mmol) of 2-C_6H_4(*t*-Bu)N=C(Me)C(Me)=N-2-C_6H_4(*t*-Bu) in 20 mL of acetonitrile. The reaction was stirred at room temperature overnight, and the solvents were removed under vacuum to give a yellow oil. The oil was redissolved in 15 mL of CH_2Cl_2 and 15 mL of hexanes. Removal of solvents in vacuo now gave 0.791 g (0.576 mmol) of a bright yellow powder (84.8% yield). Two isomers are observed in the ^{1}H NMR spectrum in an approximate 9:1 ratio, but the aryl shifts of the minor isomer are obscured. ^{1}H NMR ($CDCl_3$, 300 MHz) δ 7.58−7.50 (m, 2H, H_{aryl}), 7.27 and 7.21 (m, 2H each, H_{aryl}), 6.59 (m, 2H, H_{aryl}), 2.16 and 2.14 (minor: 2.20 and 2.18) (s, 3H each, N=C(*CH*$_3$)−C(*CH*$_3$′)=N), 1.69 (minor: 1.71) (s, 3H, NC*Me*), 1.43 and 1.41 (minor: 1.383 and 1.380) (s, 9H each, C(*CH*$_3$)$_3$), 0.57 (minor: 0.62) (s, 3H, Pd*Me*). ^{13}C{^{1}H} NMR (CD_2Cl_2, 300 MHz) (minor product not reported) δ 179.7 and 172.2 (N=*C*−*C*′=N), 144.8 and 144.0 (Ar, Ar′: C_{ipso}), 140.3 and 139.7 (Ar, Ar′: *C*-C(Me)$_3$), 129.7, 128.66, 128.64, 128.0, 127.8, 127.7, 122.5, 121.0, 120.9, 36.4, and 35.9 (*C*(Me)$_3$ and *C*′(Me)$_3$), 31.9 and 31.1 (C(*Me*)$_3$ and C′(*Me*)$_3$), 22.5 and 20.8 (N=C(*Me*)−C(*Me*′)=N), 7.7 (Pd*Me*), 1.8 (NC*Me*). Anal. Calcd for $C_{73}H_{65}N_2BF_{24}$OPd: C, 51.57; H, 3.67; N, 3.06. Found: C, 52.11; H, 3.91; N, 3.06.

(f) [[(ArN=C(Me)C(Me)=NAr)PdMe]$_2$(μ-Cl)]BAr′$_4$ (Ar = 2,6-C_6H_3(*i*-Pr)$_2$). Et_2O (25 mL) was added to a mixture of (ArN=C(Me)C(Me)=NAr)PdMeCl (0.81 g, 1.45 mmol) and 0.5 equiv of NaBAr′$_4$ (0.64 g, 0.73 mmol) at 25°C. A golden yellow solution and NaCl precipitate formed immediately upon mixing. The reaction mixture was stirred for 19 h and then filtered. After the Et_2O was removed in vacuo, the product was washed with 25 mL of hexane. The yellow powder was then dissolved in 25 mL of CH_2Cl_2, and the resulting solution was filtered in order to removed traces of unreacted NaBAr′$_4$. Removal of CH_2Cl_2 in vacuo yielded a golden yellow powder (1.25 g, 88.2%): ^{1}H NMR (CD_2Cl_2, 400 MHz) δ 7.33 (t, 2, J = 7.57 Hz, Ar: H_p), 7.27 (d, 4, J = 7.69 Hz, Ar: H_m), 7.18 (t, 2, J = 7.64 Hz, Ar: H_p), 7.10 (d, 4, J = 7.44 Hz, Ar′: H_m), 2.88 (septet, 4, J = 6.80 Hz, C*H*Me$_2$), 2.75 (septet, 4, J = 6.82 Hz, C′*H*Me$_2$), 2.05 and 2.00 (s, 6 each, N=C(*Me*)−C′(*Me*)=N), 1.22, 1.13, 1.08, and 1.01 (d, 12 each, J = 6.61−6.99 Hz, CH*MeMe*′, C′H*MeMe*′), 0.41 (s, 6, Pd*Me*); ^{13}C{^{1}H} NMR (CD_2Cl_2, 100 MHz) δ 177.1 and 171.2 (N=*C*−*C*′=N), 141.4 and 141.0 (Ar, Ar′: C_{ipso}), 138.8 and 138.1 (Ar, Ar′: C_o), 128.6 and 127.8 (Ar, Ar′: C_p), 124.5 and 123.8 (Ar, Ar′: C_m), 29.3 (*C*HMe$_2$), 29.0 (*C*′HMe$_2$), 23.8, 23.7, 23.6, and 23.0 (CH*MeMe*′, C′H*MeMe*′), 21.5 and 20.0 (N=C(*Me*)−C′(*Me*)=N), 9.8 (J_{CH} = 136.0 Hz, Pd*Me*). Anal. Calcd for ($C_{90}H_{98}BClF_{24}N_4Pd_2$): C, 55.41; H, 5.06; N, 2.87. Found: C, 55.83; H, 5.09; N, 2.63.

(g) [[(ArN=C(H)C(H)=NAr)PdMe]$_2$(μ-Cl)]BAr′$_4$ (Ar = 2,6-C_6H_3(*i*-Pr)$_2$). The above procedure was followed with one exception. The removal of CH_2Cl_2 in vacuo yielded a product that was partially an oil. Dissolving the compound in Et_2O and then removing the Et_2O in vacuo yielded a microcrystalline red solid (85.5%). ^{1}H NMR (CD_2Cl_2, 400 MHz) δ 8.20 and 8.09 (s, 2 each, N=C(*H*)−C′(*H*)=N), 7.37 (t, 2, J = 7.73 Hz, Ar: H_p), 7.28 (d, 4, J = 7.44 Hz, Ar: H_m), 7.24 (t, 2, Ar′: H_p), 7.16 (d, 4, J = 7.19 Hz, Ar′: H_m), 3.04 (septet, 4, J = 6.80 Hz, C*H*Me$_2$), 2.93 (septet, 4, J = 6.80 Hz, C′*H*Me$_2$), 1.26 (d, 12, J = 6.79 Hz, CH*Me*Me′), 1.14 (d, 12, J = 6.83 Hz, CHMe*Me*′), 1.11 (d, 12, J = 6.80 Hz, C′H*Me*Me′), 1.06 (d, 12, J = 6.79 Hz, C′HMe*Me*′), 0.74 (s, 6, Pd*Me*); ^{13}C{^{1}H} NMR (CD_2Cl_2, 100 MHz) δ 166.0 (J_{CH} = 180.4 Hz, N=*C*(H)), 160.8 (J_{CH} = 179.9 Hz, N=*C*′(H)), 143.5 and 143.0 (Ar, Ar′: C_{ipso}), 139.8 and 138.9 (Ar, Ar′: C_o), 129.3 and 128.5 (Ar, Ar′: C_p), 124.3 and 123.7 (Ar, Ar′: C_m), 29.2 and 28.9 (*C*HMe$_2$, *C*′HMe$_2$), 24.5, 24.1, 23.0, and 22.5 (CH*MeMe*′, C′H*MeMe*′), 10.3 (Pd*Me*). Anal. Calcd for ($C_{86}H_{90}BClF_{24}N_4Pd_2$): C, 54.52; H, 4.97; N, 2.96. Found: C, 54.97; H, 4.72; N, 2.71.

Intramolecular C−H Activation. (a) [ArN=C(H)C(H)=N-2,6-C_6H_3-*i*-Pr,CHMeCH$_2$Pd(OEt$_2$)]BAr′$_4$ (Ar = 2,6-C_6 H_3(*i*-Pr)$_2$), 1a′. A 700 μL CD_2Cl_2 solution of [(ArN=C(H)C(H)=NAr)PdMe(OEt$_2$)]-BAr′$_4$ (68.4 mg, 0.0477 mmol) was allowed to stand at 25 °C for several hours and then at −30 °C overnight. Such highly concentrated solutions of the resulting metallacycle were stable for hours at 25 °C. ^{1}H NMR (CD_2Cl_2, 400 MHz, 41 °C) δ 8.17 (s, 2, N=C(*H*)−C′(*H*)=N), 7.5−7.0 (m, 6, H_{aryl}), 3.48 (q, 4, J = 6.88 Hz, O(CH_2CH$_3$)$_2$), 3.26 (septet, 1, J = 6.49 Hz, C*H*Me$_2$), 3.08 (septet, 1, J = 6.86 Hz, C′*H*Me$_2$), 2.94 (septet, 1, J = 6.65 Hz, C″*H*Me$_2$), 2.70 (dd, 1, J = 6.67 Hz, 0.90, CHMeC*H*H′Pd), 2.43 (dd, 1, J = 7.12 Hz, 4.28, CHMeCH*H*′Pd), 2.23 (br m, 1, C*H*MeCH$_2$Pd), 1.54 (d, 3, J = 6.86 Hz, CH*Me*CH$_2$Pd), 1.43 (d, 3, J = 6.79 Hz, C″H*Me*Me′), 1.40 (d, 3, J = 7.12 Hz, CH*Me*Me′), 1.37 (d, 3, J = 6.95 Hz, C′H*Me*Me′), 1.27 (d, 6, J = 6.79 Hz, C′HMe*Me*′, C″HMe*Me*′), 1.12 (d, 3, J = 6.54 Hz, CHMe*Me*′), 1.23 (br m, 6, O(CH$_2$C*H*$_3$)$_2$), 0.21 (CH$_4$); ^{13}C{^{1}H} NMR (CD_2Cl_2, 100 MHz, 41 °C) δ 162.5 (J_{CH} = 181.5 Hz, N=*C*(H)), 161.2 (J_{CH} = 178.4 Hz, N=*C*′(H)), 145.8 and 144.5 (Ar, Ar′: C_{ipso}), 141.6, 140.7, 140.3, and 138.8 (Ar, Ar′: C_o, C_o′), 131.6 and 129.8 (Ar, Ar′: C_p), 128.1, 127.6, 125.2, and 124.5 (Ar, Ar′: C_m, $C_{m'}$), 72 (br, O(*C*H$_2$CH$_3$)$_2$), 43.2 (CHMe*C*H$_2$Pd), 40.5 (*C*HMeCH$_2$Pd), 29.5,. 29.1 and 28.8 (*C*HMe$_2$, *C*′HMe$_2$, *C*″HMe$_2$), 26.2 (br), 25.3, 25.2, 25.1, 24.5 (br), 23.3 and 22.1 (CH*MeMe*′, C′H*MeMe*′, C″H*MeMe*′, CH*Me*CH$_2$Pd), 15.5 (br, O(CH$_2$*C*H$_3$)$_2$), −14.8 (*C*H$_4$).

(b) Ethylene Polymerization Catalyzed by [ArN=C(H)C(H)=N-2,6-C_6H_3-*i*-Pr,CHMeCH$_2$Pd(OEt$_2$)]BAr′$_4$ (Ar = 2,6-C_6H_3-(*i*-Pr)$_2$) (1a′). Addition of ethylene to a CD_2Cl_2 solution of this compound resulted in displacement of Et_2O to give the corresponding ethylene adduct **1c′**. Warming of the ethylene adduct in the presence of excess ethylene resulted in branched polymer formation: ^{1}H NMR (CD_2Cl_2) δ 1.3 ppm (CH_2)$_n$, 0.9 ppm (CH_3). Rates of initiation were significantly slower than rates of propagation.

(c)[ArN=C(H)C(H)=N-2,6-C_6H_3-*i*-Pr,CHMeCH$_2$Pd(H$_2$C=CH$_2$)]-BAr′$_4$ (Ar = 2,6-C_6H_3-(*i*-Pr)$_2$) (1c′). ^{1}H NMR (CD_2Cl_2, 400 MHz, −61 °C) δ 8.25 and 8.23 (N=C(*H*)−C′(*H*)=N), 7.55−7.16 (m, 6, H_{aryl}), 4.67 (m, 2, *H*H′C=C*H*H′), 4.40 (m, 2, H*H*′C=CH*H*′), 2.95 (septet, 1, J = 6.30 Hz, C*H*Me$_2$), 2.80 (septet, 2, J = 6.36 Hz, C′*H*Me$_2$ and C″*H*Me$_2$), 2.53 (br m, 1, C*H*MeCH$_2$Pd), 2.43 (d, 1, J = 8.16 Hz, CHMeC*H*H′Pd), 1.73 (dd, 1, J = 8.16, 2.84 Hz, CHMeCH*H*′Pd), 1.45 and 1.19 (d, 3 each, J = 6.79−6.40 Hz, CH*MeMe*′), 1.42 (d, 3, J = 7.05 Hz, CH*Me*CH$_2$Pd), 1.30, 1.30, 1.19, and 0.99 (d, 3 each, J = 6.40−6.65 Hz, C′H*MeMe*′ and C″H*MeMe*′); ^{13}C{^{1}H} NMR (CD_2Cl_2, 100 MHz, −61 °C) δ 162.7 (J_{CH} = 179.7 Hz, N=*C*H), 162.1 (J_{CH} = 180.9 Hz, N=*C*′H), 144.7, 141.7, 141.2, 139.2, 137.5, and 137.1 (Ar, Ar′: C_{ipso}, C_o, C_o'), 131.0 and 129.0 (Ar, Ar′: C_p), 124.6 and 124.0 (Ar, Ar′: C_m), 92.3 (J_{CH} = 162.4 Hz, H_2C=*C*H$_2$), 45.1 (*C*H$_2$Pd), 41.1 (*C*HMeCH$_2$Pd), 28.9, 28.5, and 28.2 (*C*HMe$_2$, *C*′HMe$_2$, *C*″HMe$_2$), 26.1, 25.6, 25.1, 24.9, 24.6, 22.9, and 21.4 (CH*MeMe*′, C′H*MeMe*′, C″H*MeMe*′, CH*Me*CH$_2$Pd).

(d) [ArN=C(Me)C(Me)=N-C_6H_4-2-$C(CH_3)_2CH_2Pd(OEt_2)$]BAr'_4 (Ar = 2-C_6H_4(*t*-Bu)), 4b′. A solution of **4b** in $CDCl_3$ exhibited slow deactivation to **4b′** at 50 °C and gave the following spectra: ^{1}H NMR ($CDCl_3$, 300 MHz) δ 7.54 (m, 1H, H_{aryl}), 7.38 (ddd, 1H, J = 7.7, 7.6, 1.3 Hz, H_{aryl}), 7.32−7.26 (m, 1H, H_{aryl}), 7.20 (2 m, 1H each, H_{aryl}), 6.88 (dd, 1H, J = 7.9, 1.3, H_{aryl}), 6.62−6.56 (2 m, 1H each, H_{aryl}), 2.55 and 2.20 (s, 3H each, N=C(CH_3)−C(CH_3')=N), 2.26 (2 coincident s, 1H each, C(Me)$_2$*CHH′Pd*), 1.72 (s, 3H, NC*Me*), 1.40 (br s, 3H, C*Me*Me′CH_2Pd), 1.32 (s, 18H, C(*Me*)$_3$), 1.29 (br s, 3H, CMe*Me′*CH_2-Pd). ^{13}C{^{1}H} NMR ($CDCl_3$, 75 MHz) δ 173.4 and 171.8 (N=*C*−*C′*=N), 148.0 and 145.0 (Ar, Ar′: C_{ipso}), 140.7 and 140.1 (Ar, Ar′: *C*-C(Me)$_3$), 130.9, 128.5, 127.9, 127.51, 127.49, 126.7, 123.6, 120.7, 119.4, 45.9 (CMe$_2$*C*H$_2$Pd), 37.7 and 35.8 (*C*(Me)$_3$ and C_6H_4-2-*C*Me$_2$-CH_2Pd), 31.9 and 31.0 (C*MeMe′*CH_2Pd), 31.1 (C(*Me*)$_3$); 22.6 and 20.7 (N=C(*Me*)−C(*Me′*)=N), 1.9 (NC*Me*).

(e) [ArN=C(An)C(An)=N-C_6H_4-2-$C(CH_3)_2CH_2Pd(OEt_2)$]BAr'_4 (Ar = 2-C_6H_4(*t*-Bu)), 5a′. Upon sitting at 0 °C for several hours, a solution of **5a** in CH_2Cl_2 changed in color from red/orange to deep red. Removal of solvent under vacuum gave a dark red brittle solid that was scraped into a powder. The product is consistent with intramolecular C−H activation to give **5a′**. ^{1}H NMR (CD_2Cl_2, 0 °C, 300 MHz) δ 8.17 (d, 1H, J = 8.2 Hz: An: H_p), 8.10 (d, 1H, J = 8.2 Hz: An: $H_{p'}$), 7.89 (d, 1H, J = 7.4 Hz, H_{aryl}), 7.70−7.27 (m, 9H, An: $H_{p'}$, H_m, $H_{m'}$, $H_{o'}$; 5 H_{aryl}), 7.04 (dd, 1H, J = 7.5, 1.53 Hz, H_{aryl}), 6.59 (d, 1H, J = 7.2 Hz, Ar: H_o), 3.51−3.32 (br, 4H, O(*CH*$_2$CH$_3$)$_2$), 2.53 (d, 1H, J = 8.1 Hz, C(Me)$_2$C*H*H′Pd), 2.24 (d, 1H, J = 7.9 Hz, C(Me)$_2$CH*H′*Pd), 1.53 (s, 3H, C*Me*Me′CH_2Pd), 1.44 (s, 3H, CMe*Me′*CH_2-Pd), 1.38 (s, 18H, C(*Me*)$_3$), 1.33 (t, 6H, O(CH_2*CH*$_3$)$_2$.

(f) [ArN=C(An)-C(An)=N-C_6H_4-2-$C(CH_3)_2CH_2Pd(CH_2=CH_2)$]-$BAr'_4$ (Ar = 2-C_6H_4(*t*-Bu)) (5c′). Addition of 20 equiv of ethylene to **5a′** resulted in displacement of ether by ethylene. No migratory insertion was observed upon standing at 25 °C after 1 day. ^{1}H NMR (CD_2Cl_2, 0 °C, 300 MHz) δ 8.23 (d, 1H, J = 8.4 Hz, An: H_p), 8.15 (d, 1H, J = 8.4 Hz, An: $H_{p'}$), 8.07 (d, 1H, J = 7.2 Hz, H_{aryl}), 7.80 (dd, 1H, J = 7.8, 1.2 Hz, H_{aryl}), 7.72−7.41 (m, 8H, An: H_m, $H_{m'}$; 6 H_{aryl}), 6.91 (dd, 1H, J = 7.2, 1.8 Hz, H_{aryl}), 7.60 (d, 1H, J = 7.2 Hz, An: H_o), 4.92 and 4.46 (2 m, 2H each, *H*H′C=C*H*H′, H*H′*C=CH*H*−), 2.41 (d, 1H, J = 9.0 Hz, C(Me)$_2$C*H*H′Pd), 1.68 (d, 1H, J = 9.0 Hz, C(Me)$_2$CH*H′*Pd), 1.53 and 1.52 (s, 3H each, *C*(*Me*Me′)CH_2Pd and C(Me*Me′*)$_2CH_2$Pd), 1.34 (s, 9H, C(CH_3)$_3$), (5.4 (unbound C_2H_4, 3.42 (q from Et_2O), 1.14 (t from Et_2O), 0.2 (CH_4)).

General Procedure for Variable Temperature NMR Experiments. In a drybox under an argon atmosphere, an NMR tube was charged with ca. 0.01 mmol of [(ArN=C(R)C(R)=NAr)Pd(Me)(L)]-BAr'_4 (or [(ArN=C(R)C(R)=NAr)Pd−(CH(CH_2-μ-H)(CH_3))]BAr'_4). The tube was capped with a rubber septum and removed from the drybox. After securing the septum with Teflon tape and Parafilm, the tube was cooled to −78 °C. CD_2Cl_2 was added to the NMR tube via gastight syringe (700 μL) or $CDCl_2F$ was added via a 22 gauge cannula (∼600−800 μL), and the septum was rewrapped with Parafilm. The tube was shaken and warmed slightly to facilitate dissolution of the complex. After acquiring a spectrum at −80 °C, olefin or other trapping ligand was added via gastight syringe to the solution cooled to −78 °C, and the NMR tube was briefly shaken to completely dissolve the additive. The tube was then transferred to the cooled NMR probe for acquisition of spectra. The concentrations of the alkyl agostic species, trapped alkyl species, free olefin, and free trapping ligands were calculated using the BAr'_4 or *p*-acenaphthyl peaks as an internal standard.

Migratory Insertion Rates. Rates of migratory insertion were monitored for ethylene and propylene as previously described (eq 10) and are listed in Tables 1 and 2. ^{1}H NMR spectra for the initially formed ethylene complexes **3c** and **5c** and for the propylene complex **3d** are described below (spectra for **1c** and **2c** have been reported).[18]

(a) [(ArN=C(An)C(An)=NAr)Pd(CH_3)($CH_2=CH_2$)]BAr'_4 (Ar = 2,6-C_6H_3(*i*-Pr)$_2$) (3c). ^{1}H NMR (CD_2Cl_2, −80 °C, 300 MHz) δ 8.09 (d, 1H, J = 8.4 Hz, An: H_p), 8.05 (d, 1H, J = 8.4 Hz, An: $H_{p'}$), 7.55−7.39 (m, 8H, An: H_m, $H_{m'}$; 6 H_{aryl}), 6.55 (d, 1H, J = 7.2 Hz, An: H_o), 6.53 (d, 1H, J = 7.5 Hz, An: $H_{o'}$), 4.62 (br s, 4H, C_2H_4), 3.03 (septet, 2H, J = 6.9 Hz, C*H*Me$_2$), 2.96 (septet, 2H, J = 6.9 Hz, C′*H*Me$_2$), 1.34 (d, 6H, J = 6.6 Hz, CH*Me*Me′), 1.29 (d, 6H, J = 6.3 Hz, CHMe*Me′*), 0.89 (d, 6H, J = 6.6 Hz, C′H*Me*Me′), 0.82 (d, 6H, J = 6.6 Hz, C′HMe*Me′*), 0.46 (s, 3H, Pd*Me*).

(b) [(ArN=C(An)C(An)=NAr)Pd(CH_3)($CH_2=CH_2$)]BAr'_4 (Ar = 2-C_6H_4(*t*-Bu)) (5c). Complex **5a** used for the kinetic runs contained 15% deactivated palladacycle **5a′** which did not promote migratory insertion of ethylene. This was accounted for in the measurement of turnovers. ^{1}H NMR (CD_2Cl_2, −80 °C, 300 MHz) δ 8.09 (d, 1H, J = 8.7 Hz, An: H_p), 8.05 (d, 1H, J = 8.7 Hz, An: $H_{p'}$), 7.67−7.45 (m, 8H, An: H_m, $H_{m'}$; 6 H_{aryl}), 7.07 (m, 1H, H_{aryl}), 6.90 (m, 1H, H_{aryl}), 6.50 (d, 1H, J = 7.5 Hz, An: H_o), 6.40 (d, 1H, J = 7.2 Hz, An: $H_{o'}$), 4.58 (dm, 4H, J = 20.1 Hz (d), C_2H_4), 1.33 (2 overlapping s, 9H each, C(CH_3)$_3$ and C′(CH_3)$_3$), 0.52 (s, 3H, Pd*Me*).

(c) [(ArN=C(An)C(An)=NAr)Pd(CH_3)($CH_2=CH_2CH_3$)]BAr'_4 (Ar = 2,6-C_6H_3(*i*-Pr)$_2$) (3c). ^{1}H NMR (CD_2Cl_2, −80 °C, 300 MHz) δ 8.12 (d, 1H, J = 8.4 Hz, An: H_p), 8.08 (d, 1H, J = 8.4 Hz, An: $H_{p'}$), 7.57−7.41 (m, 8H, An: H_m, $H_{m'}$; 6 H_{aryl}), 6.53 (d, 1H, J = 7.2 Hz, An: H_o), 6.51 (d, 1H, J = 7.5 Hz, An: $H_{o'}$), 5.24 (m, 1H, CH_2=C*H*CH$_3$), 4.56 and 4.39 (2 br m, 2H, C*H*$_2$=CHCH$_3$), 3.12−2.92 (4 septets, 1H each, C*H*Me$_2$, C′*H*Me$_2$, C″*H*Me$_2$, and C‴*H*Me$_2$), 1.78 (s, 3H, J = 6.0 Hz, CH$_2$=CHC*H*$_3$), 1.39, 1.34−1.29 (2), 0.92, 0.89, 0.89, 0.85, and 0.83 (8 d, 3H each, J = 6.3−6.9 Hz, CH*MeMe′*, C′H*MeMe′*, C″H*MeMe′*, C‴H*MeMe′*), 0.58 (s, 3H, Pd*Me*).

Alkyl Agostic Complexes. [(ArN=C(An)C(An)=NAr)Pd(CH-(CH_2-μ-H)(CH_3))]BAr'_4 (Ar = 2,6-C_6H_3(Me)$_2$) (i-17). Synthesis of the β-agostic isopropyl complex **i-16** has been reported.[48] The β-agostic isopropyl complex **i-17** was prepared in a similar fashion: In a drybox under an argon atmosphere, an NMR tube was charged with ca. 15 mg of **6a** (ca. 1 × 10^{-5} mol). The tube was capped with a rubber septum and removed from the drybox. After securing the septum with Teflon tape and Parafilm, the tube was cooled to −78 °C. $CDCl_2F$ was added to the NMR tube via a 22 gauge cannula (∼600−800 μL), and the septum was sealed with silicon grease and rewrapped with Parafilm. The tube was shaken and warmed slightly to facilitate dissolution of the complex. After acquiring a spectrum at −80 °C, 0.95 equiv of ethylene was added via gastight syringe to the solution of **6a** cooled to −78 °C, and the NMR tube was briefly shaken to completely dissolve the olefin. The tube was then transferred to the cooled NMR probe, and migratory insertion of the methyl ethylene complex **6c** was followed at 0 °C. Formation of the desired β-agostic complex was confirmed by acquiring a spectrum at ca. −115 °C for **i-17**, which exhibited a broad triplet at −8.0 ppm, characteristic of the agostic hydrogen of a methyl group. The spectra acquired in $CDCl_2F$ described below were referenced to the ortho hydrogens of BAr'_4- at 7.71 ppm, as the residual proton shifts from the solvent were partially or completely obscured by aryl signals. ^{1}H NMR ($CDCl_2F$, −120 °C (static), 300 MHz): δ 8.25−7.93 (2 br doublets, 1H each, An: H_p and $H_{p'}$), 7.22−7.14 (br m, 8H, An: H_m, $H_{m'}$, 6 H_{aryl}), 6.70 (d, 1H, J = 8.1 Hz, An: H_o), 6.68 (d, 1H, J = 8.1 Hz, An: $H_{o'}$), 2.83 (br septet, 1H, PdC*H*(CH_2-μ-H)(CH_3)), 2.17−2.12 (4 br singlets, 3H each, 2,6-C_6H_3(*Me*,Me′), 2,6-C_6H_3-(Me,*Me′*), 2,6-C_6H_3'(*Me*,Me′), and 2,6-C_6H_3'(Me,*Me′*)), 1.38 (PdCH-(CH_2-μ-H)(CH_3)), 0.27 (br s, 3H, Pd(CH(CH_2-μ-H)(*C*H$_3$)), −7.85 (br t, 1H, J = 16 Hz, Pd(CH(CH_2-μ-*H*)(CH_3)). ^{1}H NMR ($CDCl_2F$, 0 °C (dynamic), 300 MHz): δ 8.08 (d, 1H, J = 8.7 Hz, An: H_p), 8.06 (d, 1H, J = 8.4 Hz, An: $H_{p'}$), 7.51−7.26 (m, 8H, An: H_m, $H_{m'}$, 6 H_{aryl}), 6.81 (d, 1H, J = 7.2 Hz, An: H_o), 6.78 (d, 1H, J = 7.2 Hz, An: $H_{o'}$), 2.26 (s, 6H, 2,6-C_6H_3(*Me*$_2$)), 2.23 (s, 6H, 2,6-C_6H_3'(*Me*$_2$)), −0.60 (br, 7H, PdC_3H_7).

Trapping of β-Agostic Species i-16/n-16. β-Agostic **i-16** can be isolated and stored or formed in situ.[48] Samples of **i-16** were added to or prepared in an NMR tube in either CD_2Cl_2 or $CDCl_2F$ according to the procedures described above. The β-agostic isopropyl complex was trapped with acetonitrile (**b**), ethylene (**c**), propylene (**d**), and dimethyl sulfide (**e**) (added via gastight microliter syringe) as isopropyl species at temperatures low enough to prevent isomerization to the *n*-propyl species. A temperature of −78 °C was sufficient for all trapping ligands except for propylene, which was introduced to an NMR tube cooled to −130 °C in a pentane/liquid N_2 bath. The ^{1}H NMR data for the initially trapped isopropyl complexes as well as the isomerized *n*-propyl complexes are listed below. Equilibrium constants for the trapped *n*-propyl/isopropyl species are indicated in Figure 5.

(a) [(ArN═C(An)C(An)═NAr)Pd(CH(CH$_3$)$_2$)(NCMe)]BAr′$_4$ (Ar = 2,6-C$_6$H$_3$(*i*-Pr)$_2$) (i-16b). ^{1}H NMR (CD$_2$Cl$_2$, −80 °C, 300 MHz): δ 8.11 (d, 1H, J = 6.6 Hz, An: H$_p$), 8.08 (d, 1H, J = 6.9 Hz, An: H$_p$′), 7.52−7.37 (m, 8H, An: H$_m$, H$_m$′, 6 H$_{aryl}$), 6.97 (d, 1H, J = 6.9, Hz, An: H$_o$), 6.30 (d, 1H, J = 7.2 Hz, An: H$_{o'}$), 3.15 (2 overlapping septets, 2H each, C*H*Me$_2$, C′*H*Me$_2$), 1.73 (s, 3H, NC*Me*), 1.37, 1.32, 0.98, and 0.83 (4 d, 6H each, J = 6.0, 5.7, 6.0, and 6.0 Hz, CH*Me*Me′, CHMe*Me*′, C′H*Me*Me′, C′HMe*Me*′), 0.67 (d, 6H, J = 5.7 Hz, PdCH(*CH*$_3$)$_2$), (PdC*H*(CH$_3$)$_2$ obscured).

(b) [(ArN═C(An)C(An)═NAr)Pd(CH$_2$CH$_2$CH$_3$)(NCMe)]BAr′$_4$ (Ar = 2,6-C$_6$H$_3$-(*i*-Pr)$_2$) (n-16b). ^{1}H NMR (CD$_2$Cl$_2$, −10 °C, 300 MHz): δ 8.15 (d, 1H, J = 6.0 Hz, An: H$_p$), 8.13 (d, 1H, J = 6.0 Hz, An: H$_p$′), 7.55−7.32 (m, 8H, An: H$_m$, H$_m$′, 6 H$_{aryl}$), 6.97 (d, 1H, J = 7.2, Hz, An: H$_o$), 6.47 (d, 1H, J = 7.5 Hz, An: H$_{o'}$), 3.28−3.13 (2 overlapping septets, 2H each, C*H*Me$_2$, C′*H*Me$_2$), 1.82 (s, 3H, NC*Me*), 1.43, 1.38, 1.37, and 1.05 (4 d, 6H each, J = 6.9, 6.6, 6.6, and 6.9 Hz, CH*Me*Me′, CHMe*Me*′, C′H*Me*Me′, C′HMe*Me*′), 0.91 (t, 3H, J = 6.6 Hz, PdCH$_2$CH$_2$*CH*$_3$), (Pd*CH*$_2$*CH*$_2$CH$_3$ obscured).

(c) [(ArN═C(An)C(An)═NAr)Pd(CH(CH$_3$)$_2$)(CH$_2$═CH$_2$)]BAr′4 (Ar = 2,6-C$_6$H$_3$(*i*-Pr)$_2$) (i-16c). ^{1}H NMR (CDCl$_2$F, −80 °C, 300 MHz): δ 7.92 (d, 1H, J = 9.0 Hz, An: H$_p$), 7.89 (d, 1H, J = 9.0 Hz, An: H$_p$′), 7.71 (s, 8H, BAr′$_4$: H$_o$), 7.44 (s, 4H, BAr′$_4$: H$_p$), 7.51−7.34 (m, 8H, An: H$_m$, H$_m$′, 6 H$_{aryl}$), 6.41 (d, 1H, J = 7.2, Hz, An: H$_o$), 6.19 (d, 1H, J = 7.2 Hz, An: H$_{o'}$), 4.56 (s, 4H, C$_2$*H*$_4$), 3.05 (septet, 2H, J = 6.0 Hz, C*H*Me$_2$), 2.89 (septet, 2H, J = 6.0 Hz, C′*H*Me$_2$), 2.4 (septet, 1H, J = 6.0 Hz, PdC*H*(CH$_3$)$_2$), 1.31, 1.26, and 0.75 (2 coincident) (4 d, 6H each, J = 5.7, 5.7, 5.4, and 5.4 Hz, CH*Me*Me′, CHMe*Me*′, C′H*Me*Me′, C′HMe*Me*′), 0.63 (d, 6H, J = 5.7 Hz, PdCH(*CH*$_3$)$_2$).

(d) [(ArN═C(An)C(An)═NAr)Pd(CH$_2$CH$_2$CH$_3$)(CH$_2$═CH$_2$)]-BAr′$_4$ (Ar = 2,6-C$_6$H$_3$-(*i*-Pr)$_2$) (n-16c). ^{1}H NMR (CDCl$_2$F, −60 °C, 300 MHz): δ 7.99 (d, 1H, J = 8.4 Hz, An: H$_p$), 7.95 (d, 1H, J = 8.4 Hz, An: H$_p$′), 7.53−7.37 (m, 8H, An: H$_m$, H$_m$′, 6 H$_{aryl}$), 6.51 (d, 1H, J = 7.2, Hz, An: H$_o$), 6.46 (d, 1H, J = 7.2 Hz, An: H$_{o'}$), 5.60 (s, 4H, C$_2$*H*$_4$), 3.01 (septet, 2H, J = 6.9 Hz, C*H*Me$_2$), 2.92 (septet, 2H, J = 6.6 Hz, C′*H*Me$_2$), 1.47 (t, 2H, J = 8.7 Hz, Pd*CH*$_2$CH$_2$CH$_3$), 1.35, 1.30, 0.85, and 0.82 (4 d, 6H each, J = 6.9, 6.6, 7.2, and 7.2 Hz, CH*Me*Me′, CHMe*Me*′, C′H*Me*Me′, C′HMe*Me*′), 0.47 (t, 3H, J = 7.2 Hz, PdCH$_2$-CH$_2$*CH*$_3$), (PdCH$_2$*CH*$_2$CH$_3$ obscured).

(e) [(ArN═C(An)C(An)═NAr)Pd(CH(CH$_3$)$_2$)(CH$_2$═CHCH$_3$)]-BAr′$_4$ (Ar = 2,6-C$_6$H$_3$(*i*-Pr)$_2$) (i-16d). ^{1}H NMR (CDCl$_2$F, −110 °C, 300 MHz): δ 7.88 (d, 1H, J = 8.1 Hz, An: H$_p$), 7.84 (d, 1H, J = 8.1 Hz, An: H$_p$′), 7.49−7.28 (m, 8H, An: H$_m$, H$_m$′, 6 H$_{aryl}$), 6.11 (d, 1H, J = 7.5, Hz, An: H$_o$), 6.08 (d, 1H, J = 6.9 Hz, An: H$_{o'}$), 5.08 (m, 1H, CH$_2$ = *CH*CH$_3$), 4.46−4.11 (m, 2H, *CH*$_2$═CHCH$_3$), 3.14, 3.05, 2.95, and 2.64 (4 br septets, 1H each, C*H*Me$_2$, C*H*′Me$_2$, C′*H*Me$_2$, C′*H*′Me$_2$), 2.27 (br septet, 1H, PdC*H*Me$_2$), 1.77 (br doublet, 3H, CH$_2$═CH*CH*$_3$), 1.33, 1.19, 0.80, and 0.66 (8 br doublets, 3H each CH*MeMe*′, C′H*MeMe*′, C″H*MeMe*′, C‴H*MeMe*′), 0.39 (br doublet, 6H, PdCH-(*CH*$_3$)$_2$).

(f) [(ArN═C(An)C(An)═NAr)Pd(CH$_2$CH$_2$CH$_3$)(CH$_2$═CHCH$_3$)]-BAr′$_4$ (Ar = 2,6-C$_6$H$_3$-(*i*-Pr)$_2$) (n-16d). ^{1}H NMR (CDCl$_2$F, −60 °C, 300 MHz): δ 7.97 (d, 1H, J = 8.4 Hz, An: H$_p$), 7.93 (d, 1H, J = 8.7 Hz, An: H$_p$′), 7.53−7.23 (m, 8H, An: H$_m$, H$_m$′, 6 H$_{aryl}$), 6.40 (2 coincident doublets, 1H Hz, An: H$_o$, H$_o$′), 5.30 (m, 1H, CH$_2$ = *CH*CH$_3$), 4.61 and 4.20 (m, 2H, *CH*$_2$═CHCH$_3$), 3.11−2.88 (4 septets, 1H each, C*H*Me$_2$, C′*H*Me$_2$, C″*H*Me$_2$, C‴*H*Me$_2$,), 1.80 (d, 3H, J = 6.0 Hz, CH$_2$═CH*CH*$_3$), 1.37−1.28 and 0.84−0.74 (8 overlapping doublets, 3H each CH*MeMe*′, C′H*MeMe*′, C″H*MeMe*′, C‴H*MeMe*′), 0.39 (t, 3H, J = 6.6 Hz, PdCH$_2$CH$_2$*CH*$_3$), (Pd*CH*$_2$*CH*$_2$CH$_3$ obscured).

(g) [(ArN═C(An)C(An)═NAr)Pd(CH(CH$_3$)$_2$)(SMe$_2$)]BAr′$_4$ (Ar = 2,6-C$_6$H$_3$(*i*-Pr)$_2$) (i-16e). ^{1}H NMR (CD$_2$Cl$_2$, −45 °C, 300 MHz): δ 8.09 (d, 1H, J = 8.4 Hz, An: H$_p$), 8.06 (d, 1H, J = 8.4 Hz, An: H$_p$′), 7.57−7.38 (m, 8H, An: H$_m$, H$_m$′, 6 H$_{aryl}$), 6.46 (d, 1H, J = 7.5, Hz, An: H$_o$), 6.18 (d, 1H, J = 7.5 Hz, An: H$_{o'}$), 3.15 (septet, 2H, J = 6.6 Hz, C*H*Me$_2$), 3.05 (septet, 2H, J = 6.6 Hz, C′*H*Me$_2$, 2.24 (septet, 1H, J = 6.0 Hz, PdC*H*Me$_2$), 2.04 (s, 6H, S*Me*$_2$), 1.40, 1.32, 0.85, and 0.80 (4 doublets, 6H each, J = 6.9, 6.9, 6.9, and 6.9 Hz, CH*Me*Me′, CHMe*Me*′, C′H*Me*Me′, C′HMe*Me*′), 0.68 (br doublet, 6H, PdCH(*CH*$_3$)$_2$).

(h) [(ArN═C(An)C(An)═NAr)Pd(CH$_2$CH$_2$CH$_3$)(SMe$_2$)]BAr′$_4$ (Ar = 2,6-C$_6$H$_3$⁻(*i*-Pr)$_2$) (n-16e). ^{1}H NMR (CD$_2$Cl$_2$, −60 °C, 300 MHz): δ 8.12 (d, 1H, J = 8.1 Hz, An: H$_p$), 8.09 (d, 1H, J = 8.1 Hz, An: H$_p$′), 7.56−7.34 (m, 8H, An: H$_m$, H$_m$′, 6 H$_{aryl}$), 6.70 (d, 1H, J = 7.2, Hz, An: H$_o$), 6.45 (d, 1H, J = 7.5 Hz, An: H$_{o'}$), 3.12 (septet, 2H, J = 6.9 Hz, C*H*Me$_2$), 3.0 (septet, 2H, J = 6.9 Hz, C′*H*Me$_2$), 2.05 (s, 6H, S*Me*$_2$), 1.37, 1.32, 0.93, and 0.84 (4 d, 6H each, J = 6.9, 6.6, 6.9, and 6.6 Hz, CH*Me*Me′, CHMe*Me*′, C′H*Me*Me′, C′HMe*Me*′), 0.51 (t, 3H, J = 7.2 Hz, PdCH$_2$CH$_2$*CH*$_3$), (Pd*CH*$_2$*CH*$_2$CH$_3$ obscured).

Isomerization of i-16L to n-16L. Rates were determined for isomerization of **i-16c** to **n-16c** (ethylene-trapped species) under various concentrations of ethylene by treatment of the process as a first-order reaction coming to equilibrium and based on K_{eq} = 19 at −65 °C. The process was monitored by loss of the acenaphthyl H$_{ortho}$ signal at 6.19 ppm standarized to the two acenaphthyl H$_{para}$ signals at ca. 8 ppm. Rates for isomerization of **i-16e** to **n-16e** (dimethyl sulfide-trapped species) were determined by monitoring the same integrals but in this case the process could be treated as an irreversible first-order reaction.

Ethylene Associative Exchange Rates. The rate of exchange of free and bound ethylene was determined by NMR line broadening experiments at −85 °C for [(ArN═C(R)C(R)═NAr)Pd(Me)(H$_2$C═CH$_2$)]BAr′$_4$ (R = H, An, Me; Ar = 2,6-C$_6$H$_3$-(*i*-Pr)$_2$). Samples were prepared according to the following procedure: The corresponding palladium ether adducts [(ArN═C(R)C(R)═NAr)Pd(Me)(H$_2$C═CH$_2$)]-BAr′$_4$ (R = H, An, Me; Ar = 2,6-C$_6$H$_3$-(*i*-Pr)$_2$) were weighed (∼15 mg) into a tared NMR tube in a nitrogen-filled drybox. The tube was then capped with a septum and Parafilm and cooled to −80 °C. Dry, degassed CD$_2$Cl$_2$ (700 μL) was then added to the palladium complex via gastight syringe, and the tube was shaken and warmed briefly to give a homogeneous solution. After acquiring a −85 °C NMR spectrum, ethylene was added to the solution via gastight syringe, and a second NMR spectrum was acquired at −85 °C. The molarity of the BAr′$_4$ counterion was calculated according to the moles of the ether adduct placed in the NMR tube. The molarity of the ethylene complexes and free ethylene were calculated using the BAr′$_4$ peaks as an internal standard. Line widths (w) were measured at half-height in units of hertz for complexed ethylene and were corrected for line widths (w_o) in the absence of exchange. The exchange rates were determined from the standard equation for the slow exchange approximation: $k = \pi(w - w_o)/[C_2H_4]$, where $[C_2H_4]$ is the molar concentration of free ethylene. A pulse delay of 60 s and a 30° pulse width were used. (The T_1 of free ethylene is 15 s.) These experiments were repeated twice, and the averaged rate constants are reported in Table 6.

X-ray Structure Determinations. Data were collected on a Rigaku AFC 6/S diffractometer with graphite-monochromated Mo Kα radiation (λ = 0.71073 Å) using a $\theta/2\theta$ Å scan; reflections with $I > 2.5\sigma$ were considered observed and included in subsequent calculations. The structures were solved by direct methods. Refinement was by full-matrix least squares with weights based on counter statistics. Hydrogen atoms were included in the final refinement using a riding model with thermal parameters derived from the atom to which they are bonded. Crystal data and experimental conditions are given in the Supporting Information. All computations were performed using the NRCVAX suite of programs.[77,78]

Acknowledgment. This work was supported by the National Science Foundation (CHE-9710380) and by DuPont. R.L.H. and L.K.J. thank the NSF for graduate and postdoctoral research fellowships, respectively. We also wish to thank Dr. Chi-Duen Poon for NMR technical assistance.

Supporting Information Available: Graphs for the determination of rates of migratory insertion for complex **5a** and rates of isomerization for **i-16c**/**n-16c** and **i-16e**/**n-16e**, tables of crystal data, structure solution and refinement, atomic coordinates, bond lengths and angles, and anisotropic thermal parameters (PDF). This material is available free of charge via the Internet at http://pubs.acs.org.

JA000893V

(77) Gabe, E. J.; LePage, Y.; Charland, J.-P.; Lee, F.; White, P. S. *J. Appl. Crystallogr.* **1989**, *22*, 384−387.

(78) Johnson, C. K. Technical Report No. ORNL-5138; Oak Ridge National Laboratory: Oak Radge, TN, 1976.